CIN-Like TCP13 is Essential For Plant Growth Regulation Under Dehydration Stress

Kaoru Urano (kaoru.urano@riken.jp)
RIKEN/CSRS https://orcid.org/0000-0002-4184-9065
Kyonoshin Maruyama
JIRCAS: Kokusai Norin Suisangyo Kenkyu Center
Tomotsugu Koyama
Suntory Fundation of Life Science
Nathalie Gonzalez
INRAE, Universiti de Bordeaux
Dirk Inze
VIB-UGENT Center for Plant Systems Biology: Vlaams Instituut voor Biotechnologie Department of Plant Systems Biology
Kazuko Yamaguchi-Shinozaki
The University of Tokyo: Tokyo Daigaku
Kazuo Shinozaki
RIKEN/CSRS

Research Article

Keywords: dehydration stress response, TCP transcription factor, leaf morphology, root growth, drought tolerance

Posted Date: October 11th, 2021

DOI: https://doi.org/10.21203/rs.3.rs-932741/v1

Version of Record: A version of this preprint was published at Plant Molecular Biology on January 20th, 2022. See the published version at https://doi.org/10.1007/s11103-021-01238-5.

Title

CIN-like TCP13 is essential for plant growth regulation under dehydration stress

Running head

TCP13 function in dehydration stress response

Authors

Kaoru Urano[1*], Kyonoshin Maruyama[2], Tomotsugu Koyama[3], Nathalie Gonzalez[4], Dirk Inzé[5,6], Kazuko Yamaguchi-Shinozaki[7], and Kazuo Shinozaki[1*]

Author information

Affiliations

[1]Gene Discovery Research Group, RIKEN Center for Sustainable Resource Science (CSRS), 3-1-1 Koyadai, Tsukuba, Ibaraki 305-0074, Japan

[2]Plant Biotechnology Division, Japan International Research Center for Agricultural Sciences (JIRCAS), 1-1 Ohwashi, Tsukuba, Ibaraki 305-8686, Japan

[3]Bioorganic Research Institute, Suntory Foundation for Life Sciences, Seikacho, Kyoto 619-0284, Japan

[4]INRAE, Université de Bordeaux, UMR1332 Biologie du fruit et Pathologie, F-33882 Villenave d'Ornon cedex, France

[5]Department of Plant Biotechnology and Bioinformatics, Ghent University, 9052 Ghent, Belgium

[6]VIB Center for Plant Systems Biology, 9052 Ghent, Belgium

[7]Laboratory of Plant Molecular Physiology, Graduate School of Agricultural and Life Sciences, The University of Tokyo, Bunkyo-ku, Tokyo 113-8657, Japan

Contributions

All the authors contributed to the design of the study conception. Materials were prepared and experiments were performed by K.U.. The first draft of the manuscript was written by K.U. and K.S., and all the authors commented on previous versions of the manuscript. All the authors read and approved the final manuscript.

[*]**Corresponding authors:**

Kaoru Urano and Kazuo Shinozaki

Gene Discovery Research Group, RIKEN Center for Sustainable Resource Science

3-1-1 Koyadai, Tsukuba, Ibaraki 305-0074, Japan

Tel.: +81-29-836-4359
Fax: +81-29-836-9111
E-mail: kaoru.urano@riken.jp, kazuo.shinozaki@riken.jp

Ethics declarations

Conflict of interest

The authors declare that they have no competing interests.

Text: 12,202words
Figures: 9
Supporting Figures: 7
Supporting Tables: 4
Methods: 1

Abstract

Plants modulate their shape and growth in response to environmental stress. However, regulatory mechanisms underlying the changes in shape and growth under environmental stress remain elusive. The CINCINNATA (CIN)-like TEOSINTE BRANCHED1/CYCLOIDEA/PCF (TCP) family of transcription factors (TFs) are key regulators for limiting the growth of leaves through negative effect of auxin response. Here, we report that stress-inducible CIN-like TCP13 plays a key role in inducing morphological changes in leaves and growth regulation in leaves and roots that confer dehydration stress tolerance in *Arabidopsis thaliana*. Transgenic Arabidopsis plants overexpressing *TCP13* (*35Spro::TCP13OX*) exhibited leaf rolling, and reduced leaf growth under osmotic stress. The *35Spro::TCP13OX* transgenic leaves showed decreased water loss from leaves, and enhanced dehydration tolerance compared with their control counterparts. Plants overexpressing a chimeric repressor domain SRDX-fused TCP13 (*TCP13pro::TCP13SRDX*) showed severely serrated leaves and enhanced root growth. Transcriptome analysis of *TCP13pro::TCP13SRDX* transgenic plants revealed that TCP13 affects the expression of dehydration- and abscisic acid (ABA)-regulated genes. TCP13 is also required for the expression of dehydration-inducible auxin-regulated genes, *INDOLE-3-ACETIC ACID5* (*IAA5*) and *LATERAL ORGAN BOUNDARIES* (*LOB) DOMAIN 1* (*LBD1*). Furthermore, *tcp13* knockout mutant plants showed ABA-insensitive root growth and reduced dehydration-inducible gene expression. Our findings provide new insight into the molecular mechanism of CIN-like TCP that is involved in both auxin and ABA response under dehydration stress.

Keywords: dehydration stress response, TCP transcription factor, leaf morphology, root growth, drought tolerance

Key message

A dehydration-inducible Arabidopsis *CIN-like TCP* gene, *TCP13*, acts as a key regulator of plant growth in leaves and roots under dehydration stress conditions.

INTRODUCTION

Plants are exposed to various environmental stresses, such as drought, high salt, and low temperature. To withstand these abiotic stresses, plants have evolved numerous mechanisms of adaptation. Inhibition of shoot growth under water deficit conditions is often observed, which improves water balance and stress tolerance, thus ensuring plant survival (Claeys and Inze 2013). Environmental cues such as water and nutrient availability, salt, temperature, and light conditions have profound effects on leaf and root architecture (Ding and De Smet 2013). Morphological changes in leaves and roots allow plants to acclimate to and tolerate environmental stress conditions. When the effect of environmental stress is temporary, continued restriction of growth can lead to a competitive disadvantage and unnecessary yield losses. Therefore, plants have evolved several tightly regulated mechanisms to balance growth and survival in response to severe abiotic stress conditions. Although the regulation of shoot and root growth under water deficit conditions is important for plant survival, the molecular mechanisms regulating morphological changes in these organs are not well understood.

Plants utilize transcriptional modulation to regulate the balance between growth and survival under abiotic stress conditions. Previous studies have shown that genes performing different functions are either upregulated or downregulated under stress conditions (Dubois et al. 2013; Kreps et al. 2002; Maruyama et al. 2004; Maruyama et al. 2009; Seki et al. 2002a; Seki et al. 2002b; Urano et al. 2017; Urano et al. 2009). During evolution, the number of transcription factors (TFs) involved in the adaptation of plants to complex environmental stresses has increased. Several different TF families are known to be involved in abiotic stress responses, including dehydration-responsive element-binding (DREB) protein, basic leucine zipper (bZIP) domain, ethylene-responsive element-binding factor (ERF), zinc-finger, WRKY, MYB, and basic helix-loop-helix (bHLH) families. These TFs mainly function as transcriptional activators of downstream genes involved in stress responses and tolerance (Chen et al. 2002; Kodaira et al. 2011; Schommer et al. 2008; Yamaguchi-Shinozaki and Shinozaki 2006). Recently, the results of high-throughput techniques, such as chromatin immunoprecipitation sequencing (ChIP-seq) and DNA affinity purification sequencing (DAP-seq), showed that differential binding of multiple TFs to downstream gene promoters ensures robust responsiveness of downstream genes to the environmental stimulus (O'Malley et al. 2016; Song et al. 2016; Sullivan et al. 2014).

The CINCINNATA-like (CIN-like) TEOSINTE BRANCHED1/CYCLOIDEA/PCF (TCP) TF family plays essential roles in the determination of leaf size and shape (Nath et al. 2003; Palatnik et al. 2003). TCPs harbor a conserved noncanonical bHLH domain, which mediates their binding to DNA or interaction with other proteins (Cubas et al. 1999; Kosugi and Ohashi 2002). The TCP proteins are grouped into two subclasses, class I and class II, based on

sequence similarity (Martin-Trillo and Cubas 2010). A total of 13 class I and 11 class II TCPs have been identified in *Arabidopsis thaliana*. Among the 11 class II *TCP* genes, *TCP2*, *TCP3*, *TCP4*, *TCP5*, *TCP10*, *TCP13*, *TCP17*, and *TCP24* belong to the *CIN-like TCP* family. Simultaneous disruption of multiple *CIN-like TCP* genes greatly affects leaf development (Koyama et al. 2010; Schommer et al. 2008). TCP3 directly activates the expression of *microRNA164* (*miR164*), *ASYMMETRIC LEAVES1* (*AS1*), *INDOLE-3-ACETIC ACID3/SHORT HYPOCOTYL2* (*IAA3/SHY2*), and several auxin-inducible genes including SMALL AUXIN UP RNA (*SAUR*) proteins, *PIN FORMED* (*PIN*) family of auxin efflux carriers, and LATERAL ORGAN BOUNDARIES (*LOB) DOMAIN* (*LBD*) TFs (Koyama et al. 2010). These target genes of TCP3 act as negative regulators of *CUP-SHAPED COTYLEDON* (*CUC*) genes for regulating leaf differentiation (Koyama et al. 2010). TCP4 directly activates the expression of *HAT2*, a HD-ZIP II TF to induce the maturation of leaf pavement cells via both auxin-dependent and independent pathways (Challa et al. 2019). TCP5 controls leaf margin development by regulating *KNAT3*, a *KNOTTED1*-like homeobox (*KNOX*) gene and *SAW1*, a BEL-like transcription factors (Yu et al. 2020). *CIN-like TCP* genes also regulate jasmonic acid (JA) and flavonol biosynthesis. JA biosynthesis is mediated by *Lipoxygenase2* (*LOX2*), which is upregulated by *TCP3* (Koyama et al. 2007) and *TCP4* (Schommer et al. 2008), and downregulated in *jaw-d* mutants (Schommer et al. 2008). TCP3 also interacts with the R2R3-MYB protein MYB12, which promotes flavonoid biosynthesis and represses auxin signaling (Li and Zachgo 2013). In addition, *CIN-like TCP* genes are involved in the control of axillary bud outgrowth. The *jaw-D, tcp5* and *tcp5tcp13tcp17* mutant plants show a significant reduction in the number of secondary branches (van Es et al. 2019).

The activity of five *CIN-like TCPs*, including *TCP2*, *TCP3*, *TCP4*, *TCP10*, and *TCP24*, during leaf development is tightly regulated by miR319 at the post-transcriptional level. Expression of *TCPs* carrying synonymous mutations, responsible for the resistance to miR319-mediated cleavage, causes severe defects in leaf morphology or seedling death in Arabidopsis, and the transition from compound leaves to simple leaves in tomato (*Solanum lycopersicum*) (Ori et al. 2007; Palatnik et al. 2003; Palatnik et al. 2007). The activity of CIN-like TCPs is also modulated at the protein level through protein–protein interactions. ARMADILLO BTB ARABIDOPSIS PROTEIN1 (ABAP1) interacts with TCP24 to modify its activity for the regulation of leaf cell proliferation (Masuda et al. 2008). The SWI/SNF chromatin remodeling ATPase, BRAHMA (BRM), modulates the activity of CIN-like TCPs to reduce the cytokinin sensitivity of leaves by increasing the expression of the negative cytokinin regulator, *ARABIDOPSIS RESPONSE REGULATOR16* (*ARR16*) (Efroni et al. 2013). The TCP INTERACTOR-CONTAINING EAR MOTIF PROTEIN1 (TIE1), a transcriptional repressor, as well as TOPLESS (TPL) and TIE1-ASSOCIATED RING-TYPE E3 LIGASE1 (TEAR1)

regulate leaf development by physically interacting with CIN-like TCPs (Tao et al. 2013; Zhang et al. 2017). However, the role of CIN-like TCP in the regulation of plant growth under abiotic stress conditions is not well characterized.

In this study, we show that an *Arabidopsis CIN-like TCP* gene, *TCP13*, is significantly induced by dehydration. We show that TCP13 plays important roles in regulating the growth of leaves and roots under abiotic stress. Arabidopsis plants overexpressing *TCP13* (*35Spro::TCP13OX*) exhibited leaf rolling and leaf growth inhibition, abscisic acid (ABA)-sensitive root growth, and elevated dehydration stress tolerance. Additionally, *tcp13* knockout mutant plants showed ABA-insensitive root growth and reduced dehydration-inducible gene expression, which supports the idea that *TCP13* acts downstream of ABA signaling pathway under dehydration stress. TCP13 also positively regulates the dehydration-inducible auxin-regulated genes, *IAA*5 and *LBD1*. Overall, our results suggest that TCP13 is an important component of a regulatory module that controls plant growth under dehydration stress.

MATERIALS AND METHODS

Plant materials and stress treatments

Arabidopsis thaliana ecotype Columbia (Col-0; WT) was used for the generation of transgenic lines used in this study. Unless otherwise stated, plants were grown on MS medium (Murashige and Skoog 1962), supplemented with 3% sucrose and 0.8% agar (MS-agar), or in soil (Dio Professional for grafting, Innovex Co., Ltd., Tokyo) at 22 °C under long-day conditions (a 16 h light/8 h dark photoperiod and 60 ± 10 μmol photons m^{-2} s^{-1} light intensity, as described previously (Urano et al. 2009; Urano et al. 2004)). The T-DNA insertion *tcp5* (SM_3_29639), *tcp13* (GK_182B12), and *tcp17* (SALK_148580) mutant lines were obtained from the Arabidopsis Biological Resource Center (ABRC), OH, USA, and the site of T-DNA insertion site in each of these mutants has been described previously (Koyama et al. 2007; Koyama et al. 2010). The *tcp13tcp15tcp17* triple mutant was generated by crossing the single mutants described previously (Koyama et al. 2017). To perform ABA or salt (NaCl) stress treatments, 2-week-old whole WT plants were transferred from the agar medium to water (control) or to water containing 10 μM ABA or175 mM NaCl for 3–6 h. To induce dehydration stress, whole plants were transferred on to a parafilm (Parafilm M PM999, Bemis Company, Neenah, WI) for 3–6 h (WT) or 3–8 h (*tcp*13 and WT).

Plasmid construction and plant transformation

To generate *35Spro::TCP13OX*, *35Spro::TCP5OX*, and *35Spro::TCP17OX* constructs, coding sequences (CDSs) of *TCP13*, *TCP5*, and *TCP17*, respectively, were amplified by PCR using sequence-specific primers and cloned into the *Eco*RV site of *pGKX*, as described previously

(Maruyama *et al.* 2009). To generate the *35Spro::TCP13SRDX* and *35Spro::TCP13-sGFP* constructs, the CDS of *TCP13* minus the stop codon was cloned into the *Sma*I site of *pGKX-SRDX* and *pGKX-sGFP*, respectively, as described previously (Fujita et al. 2005; Maruyama et al. 2009; Qin et al. 2008). To construct the *TCP13pro::TCP13SRDX* plasmid, the *TCP13* promoter (~1,000 bp upstream of the transcription start site) was PCR amplified and cloned into *35Spro::TCP13SRDX* between *Kpn*I and *Xba*I restriction sites. To construct the *TCP13pro::GUS* plasmid, first the *pGKX-GUS* construct was generated by cloning the *GUS* reporter gene amplified from the *pBI101* vector (Fujita et al. 2005; Maruyama et al. 2009; Qin et al. 2008; Urano et al. 2004) into the *pGKX-sGFP* plasmid between *Bam*HI and *Eco*RV restriction sites. Then, the *TCP13* promoter region was cloned into the *pGKX-GUS* plasmid between *Kpn*I and *Xba*I restriction sites. These constructs were introduced into *Agrobacterium tumefaciens* strain C58, which was then used to transform Arabidopsis plants via vacuum infiltration (Bechtold and Pelletier 1998). Seeds of T2 or T3 plants were used for subsequent experiments.

Histochemical GUS staining and GFP detection in protoplasts

Histochemical GUS staining was performed as described previously (Urano et al. 2004), and GUS was observed using an M205C stereomicroscope equipped with a DFC490 digital color camera (Leica Microsystems). To determine the subcellular localization of TCP13, plasmid DNA (5 μg) isolated from *35Spro::TCP13-sGFP* plants was transfected into Arabidopsis mesophyll protoplasts, and GFP was detected under a confocal laser scanning microscope (LSM510; Zeiss). Arabidopsis protoplast isolation and PEG-calcium transfection were performed as described previously (Yoo et al. 2007).

ABA sensitivity of transgenic and mutant plants

The ABA sensitivity test was performed using *35Spro::TCP13OX* and control plants grown in plates containing 1/2 MS medium supplemented with 1% sucrose, 30 mg/L kanamycin, and 0.8% agar or *tcp13* mutant and WT (Col-0) plants grown in plates containing half-strength MS (1/2 MS) medium supplemented with 1% sucrose and 0.8% agar at 22 °C under long-day conditions. To perform the ABA sensitivity test, 5-day-old plants were transferred to plates containing 1/2 MS medium supplemented with 1% sucrose, 1.2% agar, and ABA (0, 50, or 100 μM for *35Spro::TCP13OX* and control plants; 0, 5, or 10 μM for *tcp13* and WT plants). After 7 days of incubation, the root elongation length of 7 plants per experiment was measured.

Osmotic stress sensitivity test of transgenic and mutant plants

The osmotic stress sensitivity test was performed using the *35Spro::TCP13OX* and control plants grown in plates containing 1/2 MS medium supplemented with 1% sucrose ,30 mg/L kanamycin, and 0.8% agar or *tcp13* mutant, *tcp13tcp15tcp17* triple mutant and WT (Col-0) plants grown on1/2 MS medium supplemented with 1% sucrose and 0.8% agar at 22 °C under long-day conditions . Plates were overlaid with a nylon mesh (Prosep; pore size = 20 μm) to prevent roots from growing into the medium in a plate (diameter = 150 mm). At 9 days after sowing (DAS), when the third leaf was fully expanded, the nylon mesh was gently lifted using forceps, and seedlings were transferred to plates containing 1/2 MS medium (control) or 1/2 MS medium supplemented with 25 mM mannitol (Sigma-Aldrich). After 13 days of incubation, the leaf area of five leaves per line was measured using ImageJ.

Dehydration tolerance test

The dehydration tolerance test was performed using the *35Spro::TCP13OX* and control plants grown in soil at 22 °C under long-day conditions. One pot contained 5 plants of each line. 9 pots of *35Spro::TCP13OXa* and *b*, and 18 pots of control plants were transferred to empty tray and exposed dehydration stress by withholding watering for 14 days in 45–60 relative humidity. After dehydration treatment, plants were grown for 7 days with well-water conditions and evaluated the survival rate of plants.

Transcriptome analysis using an oligo DNA array

The Agilent Arabidopsis 4 Oligo Microarray (Agilent Technologies) containing 21,500 probes was used to identify genes downstream of *TCP13*. Total RNA was isolated from 2-week-old *TCP13pro::TCP13SRDX* whole plants using extraction buffer (0.2 M Tris-HCl [pH 9.0], 0.4 M LiCl, 25 mM EDTA, and 1% SDS). Total RNA of 10 plants of each transgenic line was pooled. This procedure was repeated to produce two biologically independent RNA pools per transgenic line. The Cy3- and Cy5-labeled cRNA of each transgenic line and control sample was hybridized to the microarray. Additionally, the color swapping experiment was performed as a technical replicate. After hybridization, the microarray slides were scanned (scanner model G2505C; scan control software version A.8.5.1; Agilent Tech, Inc., Santa Clara, CA, USA), and data were analyzed using the Feature Extraction software (version 10.10.1.1; Agilent). Raw data were analyzed using the GeneSpring GX software (version 12.0; Agilent). Expression log ratios and Benjamini-Hochberg FDR *p*-values were calculated using GeneSpring GX. The microarray design and data were deposited at ArrayExpress (accession number E-MTAB-9336).

Gene expression analysis by qRT-PCR

Gene expression was analyzed by qRT-PCR as described previously (Urano et al. 2017). The

AGI code- and gene-specific primers were designed based on the sequence of a single exon using Primer Express 2.0 (Applied Biosystems, Foster City, CA, USA) (Methods S1). All qRT-PCR reactions were performed in three technical replicates, and mRNA levels of genes were normalized relative to the constitutive control, *At2g32170*.

Transactivation analysis of the *AHG3*, *Gols2*, *IAA5*, and *LBD1* promoter

Protoplasts were isolated from peeled rosette leaves of 3–4-week-old WT and *tcp13* mutant Arabidopsis plants using the Tape Arabidopsis Sandwich method (Wu et al. 2009), as described previously (Sakamoto et al. 2016; Yoshida et al. 2013). The reporter construct containing the firefly (*Photinus pyralis*) *LUC* gene driven by the *AHG3*, *Gols2*, *IAA5*, or *LBD1* promoter was co-transfected into the WT and *tcp13* mutant protoplasts using the PEG transfection method, as described previously (Sakamoto et al. 2016; Yoshida et al. 2013), along with a construct containing the modified *Renilla reniformis* luciferase gene driven by the CaMV *35S* promoter (*phRLHSP*; internal control). The transfected protoplasts were incubated at 22°C in the dark in medium supplemented with or without 5 μM ABA or 1 μM IAA for 16–18 h. The dual-LUC assay was carried out using the Pikka Gene Dual Assay Kit (Toyo Ink, Inc., Tokyo, Japan). The reporter activity was normalized with the activity of the *Renilla* luciferase gene.

RESULTS

TCP13 shows dehydration-inducible expression

Water deficit stress induces morphological changes in plants to ensure survival. To identify key factors that control these morphological changes under dehydration stress, we analyzed the expression patterns of Arabidopsis *TCP* genes in leaves under dehydration stress using our previously published microarray data (Urano et al. 2009). Of the 24 Arabidopsis *TCP* genes on the Agilent oligo array, 11 were expressed (Fig. S1). This microarray analysis showed that only *TCP13* was upregulated under dehydration stress, whereas other *TCPs* were downregulated. The up-regulation of *TCP13* under dehydration stress is also supported by the Arabidopsis RNA-seq Database (http://ipf.sustech.edu.cn/pub/athrna/; Zhang *et al.* 2020) (Table S1).

Amino acid sequence alignment of Arabidopsis class II TCPs suggests that TCP13 is relatively similar to TCP5 and TCP17 (Fig. 1a). *TCP5*, *TCP13*, and *TCP17* do not contain the *miR319A/JAW* target sequence (Palatnik et al. 2003), and all three TCPs have been previously shown to be involved in leaf differentiation, which is a common function of CIN-like TCPs (Koyama et al. 2007; Koyama et al. 2010). Fig. 1b shows the results of quantitative real-time PCR (qRT-PCR) analysis of *TCP5*, *TCP13*, and *TCP17* in Arabidopsis plants exposed to ABA, high salt, or dehydration stress for 3 or 6 h. The expression of *TCP13* was highly upregulated during the early phase of dehydration stress, and slightly upregulated by exogenous ABA and

high salinity. In contrast, the expression of *TCP5* decreased during the early phase of dehydration. Expression of *TCP17* was not affected by any of the three abiotic stresses (Fig. 1B).

To investigate why the response of *TCP13* to abiotic stress was different from that of *TCP5* and *TCP17*, we analyzed the promoter sequences of all three genes. The *TCP13* promoter contained two typical ABRE motifs (ACGTGG) (Fig. 1c). By contrast, *TCP5* and *TCP17* promoters lacked the ABRE motif but contained an auxin-responsive element, named GMSAUR (CATATG), which was found in the promoter of an auxin-responsive gene, *SAUR15A*, of soybean (*Glycine max*) (Xu et al. 1997). These results suggest that TCP13 might perform a unique function under dehydration stress via ABA signaling. In addition, amino acid sequence alignment of class II TCPs of selected vascular land plants such as Arabidopsis, *Brassica napus*, soybean, alfalfa (*Medicago truncatula*), rice (*Oryza sativa*), maize (*Zea mays*), and a bryophyte (*Physcomitrella patens*) was shown in Fig. S2.

Tissue-specific expression of *TCP13*, and subcellular localization of TCP13 protein

To analyze the tissue-specific expression profile of *TCP13*, we performed histochemical staining of transgenic Arabidopsis plants expressing the *β-glucuronidase* (*GUS*) gene under the control of the *TCP13* promoter (*TCP13pro::GUS*) (Fig. 2a–c), and analyzed the expression of *TCP13* in leaves and roots of wild-type (WT) plants by qRT-PCR (Fig. 2d). GUS activity was detected in the leaves, but not in the roots, of 5- and 10-day-old plants (Fig. 2a and b). GUS staining was detected in cotyledon and true leaves (Fig. 2a and b). GUS staining was specifically detected in expanding cells (upper region) but not in dividing cells (lower region) in young leaves (Fig. 2c). Additionally, qRT-PCR analysis showed that the expression level of *TCP13* was high in leaves and low in roots (Fig. 2d). Tissue-specific *TCP13* expression data obtained from the Arabidopsis EFP browser (http://bar.utoronto.ca/efp/cgi-bin/efpWeb.cgi) (Winter et al. 2007) showed that *TCP13* is expressed in mesophyll cells, but not in guard cells, of leaves (Fig. S3a), and in the endodermis and cortex of roots under salt stress (Fig. S3b).

To determine the subcellular localization of TCP13, we fused the full-length *TCP13* gene to a synthetic *green fluorescent protein* (*sGFP*) gene (*TCP13-sGFP*), and introduced the construct into Arabidopsis leaf protoplasts via polyethylene glycol (PEG)-mediated transfection. The TCP13-sGFP fusion protein was transiently expressed in the nuclei (Fig. 2e). Together, these data suggest that *TCP13* exhibits strong expression in leaves, and the encoded protein localizes to the nuclei.

Characterization of *TCP13* overexpression (*TCP13OX*) lines, *TCP13* repression (*TCP13SRDX*) lines and *tcp13* loss-of-function mutant plants at different developmental stages.

First, we analyzed transgenic plants overexpressing *TCP13* cDNA under the control of the constitutive Cauliflower mosaic virus (CaMV) *35S* promoter (*35Spro::TCP13OX*). The *35Spro::TCP13OX* seedlings showed longer hypocotyls and shorter roots than plants transformed with the empty vector (control) (Fig. 3a–c). True leaves of *35Spro::TCP13OX* plants were narrower than those of control plants and showed downward rolling (Fig. 3d, e, i, and j). We also examined the effect of *TCP13* repression on plant morphology. The Chimeric REpressor Silencing Technology (CRES-T) is a gene silencing system, in which a TF fused to the EAR-motif repression domain (Leu-Asp-Leu-Asp-Leu-Glu-Leu-Arg-Leu-Gly-Phe-Ala;SRDX) dominantly represses the transcription of its target genes, regardless of the absence or presence of endogenous and functionally redundant TFs (Hiratsu et al. 2003). We generated transgenic plants expressing *SRDX*-fused *TCP13* cDNA (*TCP13SRDX*). Transgenic Arabidopsis plants expressing the chimeric repressor under the control of the constitutive CaMV 35S promoter (*35Spro::TCP13SRDX*) produced ectopic shoots and failed to grow when transferred to soil (Fig. 3f). Transgenic seedlings expressing the chimeric repressor under the control of the *TCP13* promoter (*TCP13pro::TCP13SRDX*) showed greater root growth (Fig. 3a and c) and wavy and serrated rosette leaves (Fig. 3g, m, and n) compared with control plants (Fig. 3d and j). Rosette leaves of *tcp13* mutant plants showed no severe phenotypic abnormality (Fig. 3k) compared with those of WT plants (Fig. 3l). By contrast, *tcp5tcp13tcp17* triple knockout mutant plants (*tcp5/13/17)* showed shorter petioles and smaller leaves (Fig. 3h and o), with slightly wavy and serrated margins (Fig. 3q), compared with the respective control (Fig. 3d) or WT plants (Fig. 3p and r), suggesting that *TCP13*, together with *TCP5* and *TCP17*, regulates leaf morphology.

We also generated transgenic Arabidopsis plants overexpressing *TCP5* and *TCP17* under the control of the constitutive CaMV *35S* promoter (*35Spro::TCP5OX* and *35Spro::TCP17OX*, respectively). Transgenic *35Spro::TCP5OX* and *35Spro::TCP17OX* seedlings showed longer hypocotyls than empty vector-transformed control plants (Fig. S4a). This phenotype of *35Spro::TCP5OX* and *35Spro::TCP17OX* seedlings was similar to that of transgenic seedlings overexpressing a mutant form of *TCP3* (*35Spro::mTCP3OX*), in which the target site of miR319/JAW was replaced with a non-target sequence (Koyama et al. 2007), and to that of previously generated transgenic seedlings overexpressing *TCP5* (*35Spro::TCP5OX*) (Han et al. 2019) and *TCP17* (*35Spro::TCP17OX*) (Han et al. 2019; Zhou et al. 2019). Furthermore, *TCP5*, *TCP13*, and *TCP17* were shown to play basic roles in promoting thermo-responsive hypocotyl growth by positively regulating PIF4 activity (Han *et al.* 2019; Zhou *et al.* 2019). In contrast to *35Spro::TCP13OX* plants, the *35Spro::TCP5OX* and *35Spro::TCP17OX* plants showed no change in root growth in comparison with control plants (Fig. S4b). These results suggest that inhibition of root growth is a unique function of *TCP13* among *CIN-like*

TCP genes.

TCP13 inhibits leaf and root growth in response to ABA and osmotic stress, and is involved in tolerance to dehydration stress

The *TCP13* gene is significantly induced by dehydration stress and slightly induced by high salinity and ABA treatments (Fig. 1b). To analyze the function of *TCP13* in ABA response, we examined the response of the *35Spro::TCP13OX* transgenic seedling and *tcp13* knockout mutant seedlings to the ABA treatment (Fig. 4). To carry out the ABA sensitivity test, the *35Spro::TCP13OX* and *tcp13* plants grown on agar plates for 5 days were transferred to plates containing agar supplemented with or without ABA. After 7 days, the root length of these seedlings was measured (Fig. 4c), and the root growth in the presence of ABA was compared with that in the absence of ABA (Fig. 4d). The *35Spro::TCP13OX* plants showed reduced root growth compared with control plants in the absence and presence of ABA treatment (Fig. 4a and c). The enhanced root growth retardation relative to the control plants was detected in the *35Spro::TCP13OX* plants under ABA treatment (Fig. 4d). In contrast, the WT and *tcp13* mutant plants showed similar growth in the absence of ABA, whereas the *tcp13* mutant plants showed greater root elongation than WT plants in response to ABA (Fig. 4b, c and d). These results suggest that TCP13 negatively regulates root growth in response to the ABA treatment.

To analyze the effect of *TCP13* on plant response to osmotic stress, we examined changes in the leaf growth of the *35Spro::TCP13OX*, *tcp13* and *tcp5/13/17* knockout mutant plants on agar plates under mannitol stress (Fig. 5). Nine-day-old plants were transferred to plates containing half-strength Murashige and Skoog (1/2 MS) medium or 1/2 MS medium supplemented with 25 mM mannitol, which has been shown to restrict leaf growth by approximately 50% (Skirycz et al. 2011). After 13 days, each rosette leaf was separated (Fig. 5a and d), and size of third (L3), fourth (L4) and fifth (L5) leaf in the mannitol treatment was compared with that in the control treatment (Fig. 5b, c, e, and f). The *35Spro::TCP13OX* plants showed growth retardation with smaller leaves compared with the control plants in control and mannitol conditions (Fig. 5 a and b). Especially, leaves of *35Spro::TCP13OXa* plants in the mannitol treatment showed severe rolling from the mid-point to the tip (Fig. 5a). The enhanced leaf growth retardation relative to the control plants was detected in L3-L5 of the *35Spro::TCP13OXa* and L4 of the *35Spro::TCP13OXb* plants under mannitol treatment (Fig. 5c). These results indicate that *35Spro::TCP13OX* leaves are hypersensitive to osmotic stress. On the other hand, the *tcp13* mutant plants treated with mannitol showed no significant changes in leaf growth compared with control plants (Fig. 5d-f). *tcp5/13/17* triple mutant plants showed growth retardation with smaller leaves compared with the control plants in control (L3-5) and mannitol (L4 and L5) conditions (Fig. 5e). The reduced leaf growth retardation relative to the

WT plants was detected in L4 of the *tcp5/13/17* mutant plants under mannitol treatment (Fig. 5f), indicating that *tcp5/13/17* showed insensitive response to osmotic stress. *TCP13* probably exhibit functional redundancies between *TCP5* and *17* for leaf growth regulation under osmotic stress.

We then examined the response of *35Spro::TCP13OX* plants to severe dehydration stress. Watering of *35Spro::TCP13OX* plants was withheld for 14 days, and the survival rate of plants was calculated at 7 days after rewatering. The *35Spro::TCP13OX* plants showed greater dehydration stress tolerance, as evident from the reduced downward leaf rolling phenotype and higher survival rate, than control plants (Fig. 6a). This result was consistent with a lower reduction in the water content of *35Spro::TCP13OX* plants, based on the measurement of the weight of detached leaves, than in the water content of control plants (Fig. 6b). On the other hand, detached leaves of *nced3-2* mutant plants (negative control), carrying a knockout mutation in a key gene responsible for dehydration-inducible ABA accumulation, showed a greater reduction in the water content than control plants (Fig. 6b). These results suggest that leaves of *35Spro::TCP13OX* plants show less water loss than control plants under dehydration stress.

Transcriptome analysis of *TCP13pro::TCP13SRDX* plants

To investigate the transcriptional regulation of *TCP13*, we performed microarray analysis of whole plants expressing the *TCP13pro::TCP13SRDX* and focused on genes downregulated in *TCP13pro::TCP13SRDX* plants (Fig. 7). The results showed that 555 genes were downregulated in *TCP13pro::TCP13SRDX* plants (fold-change [FC] < 0.5; $p < 0.05$; false discovery rate [FDR] < 0.0277) (Table S2) compared with control plants.

Next, we performed Gene Ontology (GO) enrichment analysis (PANTHER Classification System, https://www.arabidopsis.org/tools/go_term_enrichment.jsp) of these 555 genes to determine their potential functions. A total of 48 GO terms were significantly enriched ($p < 0.05$) (Table S3), and the top 10 categories are shown in Fig. 7a. Among these GO terms, "response to stimulus" was the most highly enriched GO term, followed by "response to abiotic stimulus" and "response to chemical". Then, we compared the 555 genes downregulated in *TCP13pro::TCP13SRDX* plants with dehydration-inducible genes reported previously (Urano *et al.* 2017). The results showed that 230 out of 555 genes were upregulated under dehydration stress in the study of Urano *et al.* (2017) (FC < 2; $p < 0.05$) (Fig. 7b). These results suggest that numerous downstream candidates of TCP13 are involved in dehydration stress response.

We further analyzed the expression of dehydration stress-responsive and ABA-regulated genes downregulated in *TCP13pro::TCP13SRDX* plants in our microarray results (Fig. 7c). These genes included *Highly ABA-induced Protein Phosphatase 2C 1* (*HAI1*), *HAI2*, *ABA-hypersensitive Germination3* (*AHG3*), *Response to Desiccation 20* (*RD20*), *RD26*, and *RD29B*,

and key genes involved in raffinose, proline, and ABA metabolism such as *Galactinol Synthase2* (*GolS2*), *delta-1-pyrroline-5-carboxylate synthase1* (*P5CS1*), and *9-cis-epoxycarotenoid dioxygenase3* (*NCED3*) (Fig. 7c). These genes were not identified as downstream candidates of CIN-like TCPs in previous studies (Koyama *et al.* 2007, 2010, 2017; Schommer *et al.* 2008) but were newly identified as downstream candidates of only the dehydration-inducible TCP13. In addition, we also found genes related to the common targets of CIN-like TCP (Koyama et al. 2007; Koyama et al. 2010; Koyama et al. 2017; Schommer et al. 2008) as being potential downstream candidates of TCP13 in our microarray results (Fig. 7d and e). These included related to JA metabolic gene and auxin-regulated genes such as *LOX2*, *IAA1*, *IAA5*, *IAA14*, *IAA17*, *IAA34*, *SAUR17*, *SAUR34*, *PIN4*, and *LBD1* (Fig. 7d), and related to flavonoid metabolic genes such as *MYB12*, *MYB111*, *Flavonol Synthase1* (*FLS1*), *FLS2*, *FLS4*, *Chalcone Isomerase* (*CHI/TT5*), *CHI-like* (*CHIL*), *flavone 3-hydroxylase* (*F3H/TT6*), *UDP-glucosyl transferase 73B2* (*UGT73B2*), and *UGT78D1* (Fig. 7e). We also analyzed the expression of ABA-regulated genes such as *AHG3*, *RD20*, *Gols2*, and *NCED3*, and auxin-regulated genes, such as *IAA5* and *LBD1*, in *35Spro*::*TCP13-OX* plants. Among these genes, *Gols2*, *NCED3*, *IAA5*, and *LBD1* were upregulated in *35Spro*::*TCP13-OX* plants compared with WT plants (Figure S8). These results revealed that expression of *TCP13SRDX* triggers changes in the expression patterns of downstream genes regulated specifically by TCP13 as well as those regulated by various CIN-like TCPs.

Furthermore, to identify common motifs present in the promoters of the top 100 most downregulated genes in *TCP13pro::TCP13SRDX* plants, we searched the frequency of hexamer motifs in 1,000 bp promoter regions (Table S4), as described previously (Maruyama et al. 2012). Among the top 10 motifs identified in gene promoters, three TCP binding motifs-related sequences (GGACCA) (Schommer et al. 2008) and four ABRE-related sequences (ACGTGG/T) (Busk and Pages 1998; Yamaguchi-Shinozaki and Shinozaki 2006) were found (Fig. 7f). Among all 555 downregulated genes, 218 genes contained the TCP binding motifs in their promoter regions, and 123 genes contained both TCP binding and ABRE motifs (Fig. 7g). The repressive activity of *TCP13* induced by the SRDX motif accurately downregulated TCP-regulated downstream genes, most of which were also responsive to ABA signaling or dehydration stress. Although many downstream candidate genes of TCP13 contained the ABRE motifs in their promoters, TCP13 probably does not directly bind to these motifs (Fig. S6). To statistically clarify the overlap between ABRE sequences (ACGTGG and ACGTGT) and TCP binding motifs (GGACCA and TGGTCC) in the promoter regions of genes downregulated by *TCP13SRDX*, we performed χ^2 tests to compare the 1,000 bp promoter region of *TCP13SRDX*-downregulated genes with that of 23,739 Arabidopsis genes previously used for motif analyses (Maruyama et al. 2012) (Fig. 7h). Significant differences were detected between the observed

and expected values of the frequency of overlap between the ABRE and TCP binding motifs in the 1,000 bp promoter regions of 218 *TCP13SRDX*-down-regulated genes. Combinations of typical ABRE sequences (ACGTGG and ACGTGT) with the TCP binding motifs (GGACCA or TGGTCC) were frequently found in the promoter regions of *TCP13SRDX*-downregulated genes. These results show that TCP13-target genes harbor both TCP binding and ABRE motifs in their promoter regions.

Genes downregulated in *tcp13* mutant plants under dehydration stress

To investigate the transcriptional regulation by TCP13 under dehydration stress conditions, the expression of genes downregulated in *TCP13pro::TCP13SRDX* plants (determined by microarray) was examined in *tcp13* mutant plants under dehydration stress by qRT-PCR (Figure 8). First, we analyzed the expression of common downstream targets of CIN-like TCPs by qRT-PCR. *IAA5* and closely related genes, *IAA19*, *LBD1*, and *LOX2*, showing reduced expression in *tcp13* mutant plants (Figure 8a). Compared with the WT, the expression of *IAA5* and *LOX2* was slightly reduced at 3 h after dehydration stress, while that of *IAA19* induction was reduced at 8 h in *tcp13* mutant plants. The expression of *LBD1* was reduced at both 3 and 8 h after dehydration stress in *tcp13* mutant plants compared with the WT. By contrast, *PIN4* and *FLS1* expression levels were reduced in *tcp13* mutant plants compared with the WT under normal conditions.

We found that dehydration-inducible expression of selected ABA-regulated genes was also reduced in *tcp13* mutant plants compared with WT plants (Figure 8b). The expression of *RD20*, *NCED3*, and *GolS2* genes was slightly reduced at 3 h after the dehydration treatment, while that of *AHG3* was reduced at 8 h after dehydration stress in *tcp13* mutant plants. We also compared the expression of *AHG3*, *RD20*, *Gols2*, and *NCED3* between ABA-treated WT and ABA-treated *tcp13* mutant plants (Figure S7). These genes were upregulated in WT plants, but those upregulations were reduced in *tcp13* mutant plants after the ABA treatment. Knockout of *TCP13* slightly reduced the response of ABA- and dehydration-inducible genes under dehydration stress. These results suggest that TCP13 is involved in the regulation of not only common target genes of CIN-like TCPs but also ABA- and dehydration-inducible genes.

Transcriptional regulation of ABA- and auxin-regulated genes by TCP13

The results of qRT-PCR analysis showed that selected ABA-regulated genes (such as *AHG3* and *Gols2*) and common target genes of CIN-like TCPs (such as *IAA5* and *LBD1*) were downregulated in *tcp13* mutant plants after dehydration stress (Fig. 8). The IAA/AUX proteins are auxin-sensitive repressors (Weijers and Wagner 2016). To clarify the effect of ABA- and auxin-regulated genes by TCP13, we selected *AHG3* and *Gols2* as the TCP-regulated ABA signaling genes and *IAA5* and *LBD1* as the TCP-regulated auxin signaling genes for reporter

assay (Fig. 9). We investigated the activity of *AHG3, Gols2*, *IAA5* and *LBD1* gene promoter fused to the *luciferase* (*LUC*) reporter in mesophyll protoplasts of WT and *tcp13* in response to the ABA and IAA treatments (Fig. 9). Fig. 9a showed the existence of three DNA binding motifs of ABRE, auxin-response elements (AuxREs) (Ulmasov et al. 1995) and TCP binding motif in the promoter regions of *AHG3, Gols2*, *IAA5* and *LBD1*. *AHG3* and *Gols2* harbor both ABRE and TCP binding motifs, whereas those of *IAA5* and *LBD1* contain three types of motifs including the ABRE, AuxRE, and TCP binding motif or TCP binding motif like. The *AHG3* and *Gols2* promoters-LUC activities increased in WT plants and those activities were reduced in the *tcp13* mutant plants after the ABA treatment (Fig. 9b). However, the activities of these promoters-LUC were not affected by the IAA treatment, indicating that *TCP13* is required for the activation of *AHG3* and *Gols2* genes during ABA signaling. *IAA5* and *LBD1* promoter-LUC activities increased in WT plants and those activity were reduced in *tcp13* mutant plants after the IAA treatment (Fig. 9c). However, the activities of these promoters-LUC were not affected by the ABA treatment, indicating that *TCP13* is required to activates *IAA5* and *LBD1* during auxin signaling.

DISCUSSION

A possible role of TCP13 in plant growth regulation in response to dehydration stress

Leaves often change their architecture and growth to cope with environmental fluctuations, such as limited water availability (Hsiao et al. 1984; Zhang et al. 2018). Leaf rolling is a spontaneous response of plants to dehydration stress. Water deficit causes downward rolling of leaves that prevents water loss and modulates the speed of plant growth in Arabidopsis (Fujita et al. 2018). However, factors regulating these morphological changes under water limiting conditions have not yet been elucidated. Identification of the genetic components that modulate leaf architecture and growth may lead to useful strategies to enhance crop yield under stress conditions.

In this study, we demonstrated that the CIN-like TCP TF, TCP13, plays a pivotal role in the regulation of plant growth under dehydration stress conditions. Among the *CIN-like TCP* gene family members, *TCP13* is significantly upregulated by dehydration stress (Fig. 1). The *TCP13* promoter contains two ABRE motifs. The *TCP13OX* transgenic Arabidopsis plants produced narrow leaves, with the downward rolling phenotype, compared with control plants, and these leaf phenotypes were drastically enhanced in response to the mannitol treatment and dehydration stress (Fig. 3, 5 and 6). Additionally, *TCP13OX* transgenic plants showed higher tolerance and reduced water loss under dehydration stress (Fig. 6). These results led us to speculate that TCP13 modulates the leaf growth to cope with dehydration stress conditions. The leaf growth retardation of the *tcp5/13/17* triple mutants were slightly reduced in response to the mannitol treatment, whereas the *tcp13* mutant plants showed no specific leaf phenotype under

548 osmotic stress conditions (Fig. 5). These observations indicate that TCP13 probably contributes
549 to the leaf growth together with TCP5 and TCP17 under stress conditions.
550 Genome-wide expression and qRT-PCR analyses revealed that *IAA1, 5, 14, 17*, and *34*
551 were repressed in *TCP13pro::TCP13SRDX* plants (Fig. 7), and dehydration-inducible
552 expression of *IAA5* and *19* was reduced in *tcp13* mutant plants under dehydration stress (Fig. 8).
553 The IAA/AUX proteins are auxin-sensitive repressors that mediate diverse physiological and
554 developmental processes in plants (Weijers and Wagner 2016). The *incurvata6* (*icu6*) semi-
555 dominant allele of the *AUXIN RESISTANT3* (*AXR3*)/*IAA17* gene increases auxin response and
556 triggers adaxial leaf rolling because of the reduced size of adaxial pavement cells, and an
557 abnormal expansion of palisade mesophyll cells (Perez-Perez et al. 2010). The downstream
558 target genes of the well-characterized TCP3 include 6 of the 29 members of the *IAA/AUX* gene
559 family as well as *IAA3/SHY2* (Koyama et al. 2010). TCP5 and TCP17 interact with PIF4 to up-
560 regulate the expression of *IAA19* and consequently regulate thermomorphogenesis, and TCP13
561 also contributes to this response (Han et al. 2019; Zhou et al. 2019). Among the 29 *IAA/AUX*
562 genes in Arabidopsis (Bargmann et al. 2013; Weijers and Wagner 2016), *IAA5*, *IAA10*, *IAA19*,
563 and *IAA31* are upregulated, whereas *IAA29* is downregulated by dehydration stress (Shani et al.
564 2017). The *IAA5, IAA6*, and *IAA19* genes are positively regulated by the DREB2A TF to
565 promote stress-induced growth inhibition required for dehydration tolerance (Shani et al. 2017).
566 Thus, we speculate that TCP13 might induces the growth inhibition through the dehydration-
567 inducible auxin repressor, *IAA5* and *19* under dehydration stress.
568 Our results showed that TCP13 is required for the expression of *LBD1* under
569 dehydration stress (Fig. 8) and in response to IAA treatment (Fig. 9). LBD1 is member of the
570 ASYMMETRIC LEAVES2 (AS2)/LOB family in Arabidopsis (Iwakawa et al. 2002). AS2
571 forms a repressor complex with ASYMMETRIC LEAVES1 (AS1) that acts directly on class I
572 *KNOX* genes (Guo et al. 2008), which promote stem cell activity and must be repressed to form
573 determinate lateral organs (Jackson et al. 1994; Long et al. 1996). AS2 also forms a protein
574 complex with CIN-like TCPs, including TCP2, 3, 4, 10, and 24, to repress the *KNOX* genes (Li
575 et al. 2012). *TCP3* transcriptionally activates *AS1* expression to repress *CUC* genes that causes
576 the repression of *KNOX* genes (Aida et al. 1999; Hibara et al. 2003; Koyama et al. 2010).
577 Additionally, AS2 forms a trimetric complex with AS1 and another LBD protein, JAGGED
578 LATERAL ORGANS (JLO), to coordinate auxin distribution and meristem function through the
579 regulation of *PIN* and *KNOX* expression in shoots and roots (Rast and Simon 2012).
580 Overexpression of the poplar (*Populus tremula* × *Populus alba*) *LBD1* ortholog (*PtaLBD1*)
581 enhances secondary phloem production in populus. Overexpression of *PtaLBD1* downregulates
582 the expression of *KNOX* genes, *ARK1* and *ARK2*, involved in vascular cambium maintenance
583 (Yordanov et al. 2010). The negative regulation of *KNOX* genes by CIN-like TCPs in a CUC-

584 dependent and -independent manner is the core process underlying the promotion of
585 differentiation of leaves (Koyama et al. 2010). Based on these reports, our results support the
586 idea that TCP13 is required for the dehydration-inducible *LBD1* expression, which potentially
587 affects the leaf development in response to dehydration stress.
588 Although an increase in ABA level and signaling has long been recognized as an
589 inhibitor of primary root growth (Antoni et al. 2013; Fujii et al. 2007; Gonzalez-Guzman et al.
590 2012; Park et al. 2009; Yoshida et al. 2010), knowledge about the underlying mechanisms is
591 incomplete. Interestingly, *tcp13* mutant plants were insensitive to the ABA treatment and
592 showed greater root growth than WT plants (Fig. 4). Additionally, *35Spro::TCP13OX* transgenic
593 seedlings showed reduced root growth compared with control plants (Fig. 3), and this reduction
594 was dramatically enhanced upon ABA treatment (Fig. 4). Moreover, *TCP13pro::TCP13SRDX*
595 transgenic seedlings showed greater root growth than control plants under normal growth
596 conditions (Fig. 3). Our transcriptome analysis showed that genes containing both ABRE and
597 TCP binding motifs in their promoter regions were significantly downregulated in
598 *TCP13pro::TCP13SRDX* plants (Fig. 7). The expression of ABA-regulated genes such as *AHG3*,
599 *RD20*, *NCED3*, and *GolS2* was reduced in *tcp13* mutant plants under dehydration stress (Fig. 8)
600 and in response to ABA treatment (Fig. 9). These results suggest that TCP13 might acts
601 downstream of ABA signaling and participates in the inhibition of root growth under stress
602 conditions. Several factors are involved in root growth inhibition via the ABA signaling pathway,
603 with auxins being of prime importance. Auxin accumulation, distribution, transport, and signal
604 transduction significantly affect primary root development (Overvoorde et al. 2010; Petricka et
605 al. 2012; Sun et al. 2018). In Arabidopsis, ABA reduces the auxin level in roots, resulting in root
606 growth arrest (Sun et al. 2018). ABA, dehydration, and PEG treatments prominently attenuate
607 the response of roots to auxin in transgenic plants expressing auxin sensor constructs such as
608 *DR5::GUS*, *IAA2pro::GUS*, and *IAA19pro::Venus* (Shani et al. 2017; Wang et al. 2011; Yang et
609 al. 2014). High concentrations of ABA decrease the expression of genes encoding auxin
610 transporters, such as AUX1 and PINs, in roots (Promchuea et al. 2017; Yang et al. 2014). ABI5
611 also suppresses *PIN1* expression, and the *abi5* mutant exhibits enhanced auxin transport in roots
612 (Yuan et al. 2014). These results suggest that ABA inhibits root development by impacting auxin
613 transport and signaling. Our transcriptome analysis showed that expression levels of *IAA5*,
614 *IAA19*, and *PIN4* were reduced in *TCP13pro::TCP13SRDX* (Fig. 7) and *tcp13* mutant plants
615 under normal growth or dehydration stress conditions (Fig. 8). Based on these reports, our
616 results support the idea that TCP13 probably contributes the root growth inhibition under
617 dehydration stress through negative regulation of auxin signaling.
618 In conclusion, the present study proposes that TCP13 might act as a positive regulator
619 of dehydration stress tolerance through regulation of ABA and auxin signaling genes. Our

results suggest that the dehydration-inducible TCP13 performs unique functions in regulating plant growth to cope with dehydration stress, and facilitates the ABA signaling. Thus, the results of this study enhance our understanding of the molecular mechanisms regulating plant growth and stress tolerance in response to dehydration stress. However, additional experiments are necessary to elucidate the detailed molecular mechanisms, especially direct regulation of ABA signaling and auxin signaling genes by TCP13. Future investigations should determine how TCP13 affect the ABA and auxin signaling genes in leaves and roots and what factors regulate the plant growth and stress tolerance through TCP13 regulation.

REFERENCES

Aida M, Ishida T, Tasaka M (1999) Shoot apical meristem and cotyledon formation during Arabidopsis embryogenesis: interaction among the CUP-SHAPED COTYLEDON and SHOOT MERISTEMLESS genes. Development 126:1563-1570

Antoni R, Gonzalez-Guzman M, Rodriguez L, Peirats-Llobet M, Pizzio GA, Fernandez MA, De Winne N, De Jaeger G, Dietrich D, Bennett MJ, Rodriguez PL (2013) PYRABACTIN RESISTANCE1-LIKE8 plays an important role for the regulation of abscisic acid signaling in root. Plant Physiol 161:931-941. https://doi.org/10.1104/pp.112.208678

Bargmann BO, Vanneste S, Krouk G, Nawy T, Efroni I, Shani E, Choe G, Friml J, Bergmann DC, Estelle M, Birnbaum KD (2013) A map of cell type-specific auxin responses. Mol Syst Biol 9:688. https://doi.org/10.1038/msb.2013.40

Bechtold N, Pelletier G (1998) In planta Agrobacterium-mediated transformation of adult Arabidopsis thaliana plants by vacuum infiltration. Methods Mol Biol 82:259-266. https://doi.org/10.1385/0-89603-391-0:259

Busk PK, Pages M (1998) Regulation of abscisic acid-induced transcription. Plant Mol Biol 37:425-435

Byrne ME (2005) Networks in leaf development. Curr Opin Plant Biol 8:59-66. https://doi.org/10.1016/j.pbi.2004.11.009

Challa KR, Rath M, Nath U (2019) The CIN-TCP transcription factors promote commitment to differentiation in Arabidopsis leaf pavement cells via both auxin-dependent and independent pathways. PLoS Genet 15:e1007988. https://doi.org/10.1371/journal.pgen.1007988

Chen W, Provart NJ, Glazebrook J, Katagiri F, Chang HS, Eulgem T, Mauch F, Luan S, Zou G, Whitham SA, Budworth PR, Tao Y, Xie Z, Chen X, Lam S, Kreps JA, Harper JF, Si-Ammour A, Mauch-Mani B, Heinlein M, Kobayashi K, Hohn T, Dangl JL, Wang X, Zhu T (2002) Expression profile matrix of Arabidopsis transcription factor genes

suggests their putative functions in response to environmental stresses. Plant Cell 14:559-574

Cheng Y, Dai X, Zhao Y (2007) Auxin synthesized by the YUCCA flavin monooxygenases is essential for embryogenesis and leaf formation in Arabidopsis. Plant Cell 19:2430-2439. https://doi.org/10.1105/tpc.107.053009

Claeys H, Inze D (2013) The agony of choice: how plants balance growth and survival under water-limiting conditions. Plant Physiol 162:1768-1779. https://doi.org/10.1104/pp.113.220921

pp.113.220921 [pii]

Cubas P, Lauter N, Doebley J, Coen E (1999) The TCP domain: a motif found in proteins regulating plant growth and development. Plant J 18:215-222

Czechowski T, Stitt M, Altmann T, Udvardi MK, Scheible WR (2005) Genome-wide identification and testing of superior reference genes for transcript normalization in Arabidopsis. Plant Physiol 139:5-17. https://doi.org/10.1104/pp.105.063743

Delarue M, Prinsen E, Onckelen HV, Caboche M, Bellini C (1998) Sur2 mutations of Arabidopsis thaliana define a new locus involved in the control of auxin homeostasis. Plant J 14:603-611. https://doi.org/10.1046/j.1365-313x.1998.00163.x

Ding Z, De Smet I (2013) Localised ABA signalling mediates root growth plasticity. Trends Plant Sci 18:533-535. https://doi.org/10.1016/j.tplants.2013.08.009

S1360-1385(13)00171-4 [pii]

Dubois M, Skirycz A, Claeys H, Maleux K, Dhondt S, De Bodt S, Vanden Bossche R, De Milde L, Yoshizumi T, Matsui M, Inze D (2013) Ethylene Response Factor6 acts as a central regulator of leaf growth under water-limiting conditions in Arabidopsis. Plant Physiol 162:319-332. https://doi.org/10.1104/pp.113.216341

pp.113.216341 [pii]

Efroni I, Han SK, Kim HJ, Wu MF, Steiner E, Birnbaum KD, Hong JC, Eshed Y, Wagner D (2013) Regulation of leaf maturation by chromatin-mediated modulation of cytokinin responses. Dev Cell 24:438-445. https://doi.org/10.1016/j.devcel.2013.01.019

S1534-5807(13)00067-1 [pii]

Fujii H, Verslues PE, Zhu JK (2007) Identification of two protein kinases required for abscisic acid regulation of seed germination, root growth, and gene expression in Arabidopsis. Plant Cell 19:485-494. https://doi.org/10.1105/tpc.106.048538

Fujita M, Tanabata T, Urano K, Kikuchi S, Shinozaki K (2018) RIPPS: A Plant Phenotyping System for Quantitative Evaluation of Growth Under Controlled Environmental Stress Conditions. Plant Cell Physiol 59:2030-2038. https://doi.org/10.1093/pcp/pcy122

Fujita Y, Fujita M, Satoh R, Maruyama K, Parvez MM, Seki M, Hiratsu K, Ohme-Takagi M,

692 Shinozaki K, Yamaguchi-Shinozaki K (2005) AREB1 is a transcription activator of
693 novel ABRE-dependent ABA signaling that enhances drought stress tolerance in
694 Arabidopsis. Plant Cell 17:3470-3488. https://doi.org/10.1105/tpc.105.035659
695 Gonzalez-Guzman M, Pizzio GA, Antoni R, Vera-Sirera F, Merilo E, Bassel GW, Fernandez
696 MA, Holdsworth MJ, Perez-Amador MA, Kollist H, Rodriguez PL (2012) Arabidopsis
697 PYR/PYL/RCAR receptors play a major role in quantitative regulation of stomatal
698 aperture and transcriptional response to abscisic acid. Plant Cell 24:2483-2496.
699 https://doi.org/10.1105/tpc.112.098574
700 Guo M, Thomas J, Collins G, Timmermans MC (2008) Direct repression of KNOX loci by the
701 ASYMMETRIC LEAVES1 complex of Arabidopsis. Plant Cell 20:48-58.
702 https://doi.org/10.1105/tpc.107.056127
703 Han X, Yu H, Yuan R, Yang Y, An F, Qin G (2019) Arabidopsis Transcription Factor TCP5
704 Controls Plant Thermomorphogenesis by Positively Regulating PIF4 Activity. iScience
705 15:611-622. https://doi.org/S2589-0042(19)30102-6 [pii]
706 10.1016/j.isci.2019.04.005
707 Hibara K, Takada S, Tasaka M (2003) CUC1 gene activates the expression of SAM-related
708 genes to induce adventitious shoot formation. Plant J 36:687-696.
709 https://doi.org/10.1046/j.1365-313x.2003.01911.x
710 Hiratsu K, Matsui K, Koyama T, Ohme-Takagi M (2003) Dominant repression of target genes
711 by chimeric repressors that include the EAR motif, a repression domain, in Arabidopsis.
712 Plant J 34:733-739. https://doi.org/1759 [pii]
713 Hsiao TC, O'Toole J C, Yambao EB, Turner NC (1984) Influence of Osmotic Adjustment on
714 Leaf Rolling and Tissue Death in Rice (Oryza sativa L.). Plant Physiol 75:338-341.
715 https://doi.org/10.1104/pp.75.2.338
716 Iwakawa H, Ueno Y, Semiarti E, Onouchi H, Kojima S, Tsukaya H, Hasebe M, Soma T, Ikezaki
717 M, Machida C, Machida Y (2002) The ASYMMETRIC LEAVES2 gene of Arabidopsis
718 thaliana, required for formation of a symmetric flat leaf lamina, encodes a member of a
719 novel family of proteins characterized by cysteine repeats and a leucine zipper. Plant
720 Cell Physiol 43:467-478. https://doi.org/10.1093/pcp/pcf077
721 Jackson D, Veit B, Hake S (1994) Expression of maize KNOTTED1 related homeobox genes in
722 the shoot apical meristem predicts patterns of morphogenesis in the vegetative shoot.
723 Development 120:405-413. https://doi.org/10.1242/dev.120.2.405
724 Kodaira KS, Qin F, Tran LS, Maruyama K, Kidokoro S, Fujita Y, Shinozaki K, Yamaguchi-
725 Shinozaki K (2011) Arabidopsis Cys2/His2 zinc-finger proteins AZF1 and AZF2
726 negatively regulate abscisic acid-repressive and auxin-inducible genes under abiotic
727 stress conditions. Plant Physiol 157:742-756. https://doi.org/10.1104/pp.111.182683

728 pp.111.182683 [pii]
729 Kosugi S, Ohashi Y (2002) DNA binding and dimerization specificity and potential targets for
730 the TCP protein family. Plant J 30:337-348. https://doi.org/1294 [pii]
731 Koyama T, Furutani M, Tasaka M, Ohme-Takagi M (2007) TCP transcription factors control the
732 morphology of shoot lateral organs via negative regulation of the expression of
733 boundary-specific genes in Arabidopsis. Plant Cell 19:473-484.
734 https://doi.org/tpc.106.044792 [pii]
735 10.1105/tpc.106.044792
736 Koyama T, Mitsuda N, Seki M, Shinozaki K, Ohme-Takagi M (2010) TCP transcription factors
737 regulate the activities of ASYMMETRIC LEAVES1 and miR164, as well as the auxin
738 response, during differentiation of leaves in Arabidopsis. Plant Cell 22:3574-3588.
739 https://doi.org/10.1105/tpc.110.075598
740 tpc.110.075598 [pii]
741 Koyama T, Sato F, Ohme-Takagi M (2017) Roles of miR319 and TCP Transcription Factors in
742 Leaf Development. Plant Physiol 175:874-885. https://doi.org/10.1104/pp.17.00732
743 Kreps JA, Wu Y, Chang HS, Zhu T, Wang X, Harper JF (2002) Transcriptome changes for
744 Arabidopsis in response to salt, osmotic, and cold stress. Plant Physiol 130:2129-2141.
745 https://doi.org/10.1104/pp.008532
746 Kumar S, Stecher G, Li M, Knyaz C, Tamura K (2018) MEGA X: Molecular Evolutionary
747 Genetics Analysis across Computing Platforms. Mol Biol Evol 35:1547-1549.
748 https://doi.org/10.1093/molbev/msy096
749 Li S, Zachgo S (2013) TCP3 interacts with R2R3-MYB proteins, promotes flavonoid
750 biosynthesis and negatively regulates the auxin response in Arabidopsis thaliana. Plant J
751 76:901-913. https://doi.org/10.1111/tpj.12348
752 Li Z, Li B, Shen WH, Huang H, Dong A (2012) TCP transcription factors interact with AS2 in
753 the repression of class-I KNOX genes in Arabidopsis thaliana. Plant J 71:99-107.
754 https://doi.org/10.1111/j.1365-313X.2012.04973.x
755 Liscum E, Reed JW (2002) Genetics of Aux/IAA and ARF action in plant growth and
756 development. Plant Mol Biol 49:387-400
757 Long JA, Moan EI, Medford JI, Barton MK (1996) A member of the KNOTTED class of
758 homeodomain proteins encoded by the STM gene of Arabidopsis. Nature 379:66-69.
759 https://doi.org/10.1038/379066a0
760 Martin-Trillo M, Cubas P (2010) TCP genes: a family snapshot ten years later. Trends Plant Sci
761 15:31-39. https://doi.org/10.1016/j.tplants.2009.11.003
762 S1360-1385(09)00287-8 [pii]
763 Maruyama K, Sakuma Y, Kasuga M, Ito Y, Seki M, Goda H, Shimada Y, Yoshida S, Shinozaki

764 K, Yamaguchi-Shinozaki K (2004) Identification of cold-inducible downstream genes
765 of the Arabidopsis DREB1A/CBF3 transcriptional factor using two microarray systems.
766 Plant J 38:982-993. https://doi.org/10.1111/j.1365-313X.2004.02100.x
767 TPJ2100 [pii]
768 Maruyama K, Takeda M, Kidokoro S, Yamada K, Sakuma Y, Urano K, Fujita M, Yoshiwara K,
769 Matsukura S, Morishita Y, Sasaki R, Suzuki H, Saito K, Shibata D, Shinozaki K,
770 Yamaguchi-Shinozaki K (2009) Metabolic pathways involved in cold acclimation
771 identified by integrated analysis of metabolites and transcripts regulated by DREB1A
772 and DREB2A. Plant Physiol 150:1972-1980. https://doi.org/10.1104/pp.109.135327
773 pp.109.135327 [pii]
774 Maruyama K, Todaka D, Mizoi J, Yoshida T, Kidokoro S, Matsukura S, Takasaki H, Sakurai T,
775 Yamamoto YY, Yoshiwara K, Kojima M, Sakakibara H, Shinozaki K, Yamaguchi-
776 Shinozaki K (2012) Identification of cis-acting promoter elements in cold- and
777 dehydration-induced transcriptional pathways in Arabidopsis, rice, and soybean. DNA
778 Res 19:37-49. https://doi.org/10.1093/dnares/dsr040
779 dsr040 [pii]
780 Masuda HP, Cabral LM, De Veylder L, Tanurdzic M, de Almeida Engler J, Geelen D, Inze D,
781 Martienssen RA, Ferreira PC, Hemerly AS (2008) ABAP1 is a novel plant Armadillo
782 BTB protein involved in DNA replication and transcription. EMBO J 27:2746-2756.
783 https://doi.org/10.1038/emboj.2008.191
784 emboj2008191 [pii]
785 Nath U, Crawford BC, Carpenter R, Coen E (2003) Genetic control of surface curvature.
786 Science 299:1404-1407. https://doi.org/10.1126/science.1079354
787 299/5611/1404 [pii]
788 O'Malley RC, Huang SC, Song L, Lewsey MG, Bartlett A, Nery JR, Galli M, Gallavotti A,
789 Ecker JR (2016) Cistrome and Epicistrome Features Shape the Regulatory DNA
790 Landscape. Cell 165:1280-1292. https://doi.org/10.1016/j.cell.2016.04.038
791 Ori N, Cohen AR, Etzioni A, Brand A, Yanai O, Shleizer S, Menda N, Amsellem Z, Efroni I,
792 Pekker I, Alvarez JP, Blum E, Zamir D, Eshed Y (2007) Regulation of LANCEOLATE
793 by miR319 is required for compound-leaf development in tomato. Nat Genet 39:787-
794 791. https://doi.org/ng2036 [pii]
795 10.1038/ng2036
796 Overvoorde P, Fukaki H, Beeckman T (2010) Auxin control of root development. Cold Spring
797 Harb Perspect Biol 2:a001537. https://doi.org/10.1101/cshperspect.a001537
798 Palatnik JF, Allen E, Wu X, Schommer C, Schwab R, Carrington JC, Weigel D (2003) Control
799 of leaf morphogenesis by microRNAs. Nature 425:257-263.

https://doi.org/10.1038/nature01958
nature01958 [pii]
Palatnik JF, Wollmann H, Schommer C, Schwab R, Boisbouvier J, Rodriguez R, Warthmann N, Allen E, Dezulian T, Huson D, Carrington JC, Weigel D (2007) Sequence and expression differences underlie functional specialization of Arabidopsis microRNAs miR159 and miR319. Dev Cell 13:115-125. https://doi.org/S1534-5807(07)00159-1 [pii]
10.1016/j.devcel.2007.04.012
Park SY, Fung P, Nishimura N, Jensen DR, Fujii H, Zhao Y, Lumba S, Santiago J, Rodrigues A, Chow TF, Alfred SE, Bonetta D, Finkelstein R, Provart NJ, Desveaux D, Rodriguez PL, McCourt P, Zhu JK, Schroeder JI, Volkman BF, Cutler SR (2009) Abscisic acid inhibits type 2C protein phosphatases via the PYR/PYL family of START proteins. Science 324:1068-1071. https://doi.org/10.1126/science.1173041
Perez-Perez JM, Candela H, Robles P, Lopez-Torrejon G, del Pozo JC, Micol JL (2010) A role for AUXIN RESISTANT3 in the coordination of leaf growth. Plant Cell Physiol 51:1661-1673. https://doi.org/10.1093/pcp/pcq123
Petricka JJ, Winter CM, Benfey PN (2012) Control of Arabidopsis root development. Annu Rev Plant Biol 63:563-590. https://doi.org/10.1146/annurev-arplant-042811-105501
Promchuea S, Zhu Y, Chen Z, Zhang J, Gong Z (2017) ARF2 coordinates with PLETHORAs and PINs to orchestrate ABA-mediated root meristem activity in Arabidopsis. J Integr Plant Biol 59:30-43. https://doi.org/10.1111/jipb.12506
Qin F, Sakuma Y, Tran LS, Maruyama K, Kidokoro S, Fujita Y, Fujita M, Umezawa T, Sawano Y, Miyazono K, Tanokura M, Shinozaki K, Yamaguchi-Shinozaki K (2008) Arabidopsis DREB2A-interacting proteins function as RING E3 ligases and negatively regulate plant drought stress-responsive gene expression. Plant Cell 20:1693-1707. https://doi.org/10.1105/tpc.107.057380
tpc.107.057380 [pii]
Rast MI, Simon R (2012) Arabidopsis JAGGED LATERAL ORGANS acts with ASYMMETRIC LEAVES2 to coordinate KNOX and PIN expression in shoot and root meristems. Plant Cell 24:2917-2933. https://doi.org/10.1105/tpc.112.099978
Romano CP, Robson PR, Smith H, Estelle M, Klee H (1995) Transgene-mediated auxin overproduction in Arabidopsis: hypocotyl elongation phenotype and interactions with the hy6-1 hypocotyl elongation and axr1 auxin-resistant mutants. Plant Mol Biol 27:1071-1083. https://doi.org/10.1007/bf00020881
Sakamoto S, Takata N, Oshima Y, Yoshida K, Taniguchi T, Mitsuda N (2016) Wood reinforcement of poplar by rice NAC transcription factor. Sci Rep 6:19925.

https://doi.org/10.1038/srep19925
srep19925 [pii]
Schommer C, Palatnik JF, Aggarwal P, Chetelat A, Cubas P, Farmer EE, Nath U, Weigel D (2008) Control of jasmonate biosynthesis and senescence by miR319 targets. PLoS Biol 6:e230. https://doi.org/10.1371/journal.pbio.0060230
07-PLBI-RA-0598 [pii]
Seki M, Ishida J, Narusaka M, Fujita M, Nanjo T, Umezawa T, Kamiya A, Nakajima M, Enju A, Sakurai T, Satou M, Akiyama K, Yamaguchi-Shinozaki K, Carninci P, Kawai J, Hayashizaki Y, Shinozaki K (2002a) Monitoring the expression pattern of around 7,000 Arabidopsis genes under ABA treatments using a full-length cDNA microarray. Funct Integr Genomics 2:282-291. https://doi.org/10.1007/s10142-002-0070-6
Seki M, Narusaka M, Ishida J, Nanjo T, Fujita M, Oono Y, Kamiya A, Nakajima M, Enju A, Sakurai T, Satou M, Akiyama K, Taji T, Yamaguchi-Shinozaki K, Carninci P, Kawai J, Hayashizaki Y, Shinozaki K (2002b) Monitoring the expression profiles of 7000 Arabidopsis genes under drought, cold and high-salinity stresses using a full-length cDNA microarray. Plant J 31:279-292. https://doi.org/1359 [pii]
Shani E, Salehin M, Zhang Y, Sanchez SE, Doherty C, Wang R, Mangado CC, Song L, Tal I, Pisanty O, Ecker JR, Kay SA, Pruneda-Paz J, Estelle M (2017) Plant Stress Tolerance Requires Auxin-Sensitive Aux/IAA Transcriptional Repressors. Curr Biol 27:437-444. https://doi.org/10.1016/j.cub.2016.12.016
Skirycz A, Claeys H, De Bodt S, Oikawa A, Shinoda S, Andriankaja M, Maleux K, Eloy NB, Coppens F, Yoo SD, Saito K, Inze D (2011) Pause-and-stop: the effects of osmotic stress on cell proliferation during early leaf development in Arabidopsis and a role for ethylene signaling in cell cycle arrest. Plant Cell 23:1876-1888. https://doi.org/10.1105/tpc.111.084160
tpc.111.084160 [pii]
Song L, Huang SC, Wise A, Castanon R, Nery JR, Chen H, Watanabe M, Thomas J, Bar-Joseph Z, Ecker JR (2016) A transcription factor hierarchy defines an environmental stress response network. Science 354. https://doi.org/aag1550 [pii]
354/6312/aag1550 [pii]
10.1126/science.aag1550
Sullivan AM, Arsovski AA, Lempe J, Bubb KL, Weirauch MT, Sabo PJ, Sandstrom R, Thurman RE, Neph S, Reynolds AP, Stergachis AB, Vernot B, Johnson AK, Haugen E, Sullivan ST, Thompson A, Neri FV, 3rd, Weaver M, Diegel M, Mnaimneh S, Yang A, Hughes TR, Nemhauser JL, Queitsch C, Stamatoyannopoulos JA (2014) Mapping and dynamics of regulatory DNA and transcription factor networks in A. thaliana. Cell Rep 8:2015-

2030. https://doi.org/10.1016/j.celrep.2014.08.019
Sun LR, Wang YB, He SB, Hao FS (2018) Mechanisms for Abscisic Acid Inhibition of Primary Root Growth. Plant Signal Behav 13:e1500069. https://doi.org/10.1080/15592324.2018.1500069
Tao Q, Guo D, Wei B, Zhang F, Pang C, Jiang H, Zhang J, Wei T, Gu H, Qu LJ, Qin G (2013) The TIE1 transcriptional repressor links TCP transcription factors with TOPLESS/TOPLESS-RELATED corepressors and modulates leaf development in Arabidopsis. Plant Cell 25:421-437. https://doi.org/10.1105/tpc.113.109223
tpc.113.109223 [pii]
Teale WD, Paponov IA, Palme K (2006) Auxin in action: signalling, transport and the control of plant growth and development. Nat Rev Mol Cell Biol 7:847-859. https://doi.org/10.1038/nrm2020
Ulmasov T, Liu ZB, Hagen G, Guilfoyle TJ (1995) Composite structure of auxin response elements. Plant Cell 7:1611-1623. https://doi.org/10.1105/tpc.7.10.1611
7/10/1611 [pii]
Urano K, Maruyama K, Jikumaru Y, Kamiya Y, Yamaguchi-Shinozaki K, Shinozaki K (2017) Analysis of plant hormone profiles in response to moderate dehydration stress. Plant J 90:17-36. https://doi.org/10.1111/tpj.13460
Urano K, Maruyama K, Ogata Y, Morishita Y, Takeda M, Sakurai N, Suzuki H, Saito K, Shibata D, Kobayashi M, Yamaguchi-Shinozaki K, Shinozaki K (2009) Characterization of the ABA-regulated global responses to dehydration in Arabidopsis by metabolomics. Plant J 57:1065-1078. https://doi.org/10.1111/j.1365-313X.2008.03748.x
TPJ3748 [pii]
Urano K, Yoshiba Y, Nanjo T, Ito T, Yamaguchi-Shinozaki K, Shinozaki K (2004) Arabidopsis stress-inducible gene for arginine decarboxylase AtADC2 is required for accumulation of putrescine in salt tolerance. Biochem Biophys Res Commun 313:369-375. https://doi.org/S0006291X03024744 [pii]
10.1016/j.bbrc.2003.11.119
van Es SW, van der Auweraert EB, Silveira SR, Angenent GC, van Dijk ADJ, Immink RGH (2019) Comprehensive phenotyping reveals interactions and functions of Arabidopsis thaliana TCP genes in yield determination. Plant J 99:316-328. https://doi.org/10.1111/tpj.14326
Vanneste S, Friml J (2009) Auxin: a trigger for change in plant development. Cell 136:1005-1016. https://doi.org/10.1016/j.cell.2009.03.001
Wang L, Hua D, He J, Duan Y, Chen Z, Hong X, Gong Z (2011) Auxin Response Factor2 (ARF2) and its regulated homeodomain gene HB33 mediate abscisic acid response in

908 Arabidopsis. PLoS Genet 7:e1002172. https://doi.org/10.1371/journal.pgen.1002172
909 Weijers D, Wagner D (2016) Transcriptional Responses to the Auxin Hormone. Annu Rev Plant
910 Biol 67:539-574. https://doi.org/10.1146/annurev-arplant-043015-112122
911 Winter D, Vinegar B, Nahal H, Ammar R, Wilson GV, Provart NJ (2007) An "Electronic
912 Fluorescent Pictograph" browser for exploring and analyzing large-scale biological data
913 sets. PLoS One 2:e718. https://doi.org/10.1371/journal.pone.0000718
914 Wu FH, Shen SC, Lee LY, Lee SH, Chan MT, Lin CS (2009) Tape-Arabidopsis Sandwich - a
915 simpler Arabidopsis protoplast isolation method. Plant Methods 5:16.
916 https://doi.org/10.1186/1746-4811-5-16
917 Xu NF, Hagen G, Guilfoyle T (1997) Multiple auxin response modules in the soybean SAUR
918 15A promoter. Plant Science 126:193-201. https://doi.org/Doi 10.1016/S0168-
919 9452(97)00110-6
920 Yamaguchi-Shinozaki K, Shinozaki K (2006) Transcriptional regulatory networks in cellular
921 responses and tolerance to dehydration and cold stresses. Annu Rev Plant Biol 57:781-
922 803. https://doi.org/10.1146/annurev.arplant.57.032905.105444
923 Yang L, Zhang J, He J, Qin Y, Hua D, Duan Y, Chen Z, Gong Z (2014) ABA-mediated ROS in
924 mitochondria regulate root meristem activity by controlling PLETHORA expression in
925 Arabidopsis. PLoS Genet 10:e1004791. https://doi.org/10.1371/journal.pgen.1004791
926 Yoo SD, Cho YH, Sheen J (2007) Arabidopsis mesophyll protoplasts: a versatile cell system for
927 transient gene expression analysis. Nat Protoc 2:1565-1572.
928 https://doi.org/10.1038/nprot.2007.199
929 Yordanov YS, Regan S, Busov V (2010) Members of the LATERAL ORGAN BOUNDARIES
930 DOMAIN transcription factor family are involved in the regulation of secondary growth
931 in Populus. Plant Cell 22:3662-3677. https://doi.org/10.1105/tpc.110.078634
932 Yoshida K, Sakamoto S, Kawai T, Kobayashi Y, Sato K, Ichinose Y, Yaoi K, Akiyoshi-Endo M,
933 Sato H, Takamizo T, Ohme-Takagi M, Mitsuda N (2013) Engineering the Oryza sativa
934 cell wall with rice NAC transcription factors regulating secondary wall formation. Front
935 Plant Sci 4:383. https://doi.org/10.3389/fpls.2013.00383
936 Yoshida T, Fujita Y, Sayama H, Kidokoro S, Maruyama K, Mizoi J, Shinozaki K, Yamaguchi-
937 Shinozaki K (2010) AREB1, AREB2, and ABF3 are master transcription factors that
938 cooperatively regulate ABRE-dependent ABA signaling involved in drought stress
939 tolerance and require ABA for full activation. Plant J 61:672-685.
940 https://doi.org/10.1111/j.1365-313X.2009.04092.x
941 Yu H, Zhang L, Wang W, Tian P, Wang W, Wang K, Gao Z, Liu S, Zhang Y, Irish VF, Huang T
942 (2020) TCP5 controls leaf margin development by regulating KNOX and BEL-like
943 transcription factors in Arabidopsis. Journal of Experimental Botany 72:1809-1821.

https://doi.org/10.1093/jxb/eraa569
Yuan TT, Xu HH, Zhang KX, Guo TT, Lu YT (2014) Glucose inhibits root meristem growth via ABA INSENSITIVE 5, which represses PIN1 accumulation and auxin activity in Arabidopsis. Plant Cell Environ 37:1338-1350. https://doi.org/10.1111/pce.12233
Zhang J, Wei B, Yuan R, Wang J, Ding M, Chen Z, Yu H, Qin G (2017) The Arabidopsis RING-Type E3 Ligase TEAR1 Controls Leaf Development by Targeting the TIE1 Transcriptional Repressor for Degradation. Plant Cell 29:243-259. https://doi.org/10.1105/tpc.16.00771
tpc.16.00771 [pii]
Zhang J, Zhang H, Srivastava AK, Pan Y, Bai J, Fang J, Shi H, Zhu JK (2018) Knockdown of Rice MicroRNA166 Confers Drought Resistance by Causing Leaf Rolling and Altering Stem Xylem Development. Plant Physiol 176:2082-2094. https://doi.org/10.1104/pp.17.01432
Zhao Y, Christensen SK, Fankhauser C, Cashman JR, Cohen JD, Weigel D, Chory J (2001) A role for flavin monooxygenase-like enzymes in auxin biosynthesis. Science 291:306-309. https://doi.org/10.1126/science.291.5502.306
Zhou Y, Xun Q, Zhang D, Lv M, Ou Y, Li J (2019) TCP Transcription Factors Associate with PHYTOCHROME INTERACTING FACTOR 4 and CRYPTOCHROME 1 to Regulate Thermomorphogenesis in Arabidopsis thaliana. iScience 15:600-610. https://doi.org/S2589-0042(19)30099-9 [pii]
10.1016/j.isci.2019.04.002

ACCESSION NUMBERS

Microarray design and data were deposited at ArrayExpress (accession no. E-MTAB-9336).

ACKNOWLEDGMENTS

We thank Kyoko Yoshiwara (JIRCAS) for microarray analysis, and Dr. Yasunari Fujita (JIRCAS) for providing the DNA of *AREB1*, active form of *AREB1* (*AREB1ΔQT)*, and *RD29B* promoter for transactivation assays. We also thank Saho Mizukado, Hiroko Kobayashi, Kumiko Matsuo, Michie Etoh, and Dr. Fuyuko Shimoda for technical assistance.

FUNDING

This research was supported by the Program for Promotion of Basic and Applied Researches for Innovations in Bio-oriented Industry (BRAIN; to K.S.); the Ministry of Agriculture, Forestry, and Fisheries (MAFF); and the Ministry of Education, Culture, Sports, Science and Technology (MEXT)/JSPS KAKENHI (20K05833 to K.U.).

980
981 **SUPPORTING INFORMATION**
982 **Fig. S1** Microarray analysis of temporal changes in the expression patterns of Arabidopsis *TCP*
983 genes.
984 **Fig. S2** Phylogenetic analysis of dicot, monocot and moss class II TCPs.
985 **Fig. S3** Expression analysis of *TCP13* in leaves and roots of Arabidopsis plants using publicly
986 available data.
987 **Fig. S4** Hypocotyl and root lengths of transgenic Arabidopsis plants overexpressing *TCP5*,
988 *TCP13*, or *TCP17* under the control of the constitutive *35S* promoter.
989 **Fig. S5** Expression analysis of downstream target genes of TCP13 in *35Spro::TCP13OX* plants
990 by qRT-PCR.
991 **Fig. S6** Analysis of the activation of the *RD29B* by TCP13.
992 **Fig. S7** Expression analysis of downstream target genes of TCP13 in ABA-treated *tcp13* mutant
993 plants by qRT-PCR.
994 **Table S1** Expression analysis of Arabidopsis *TCP* genes under dehydration stress using data
995 available from the Arabidopsis RNA-seq Database.
996 **Table S2** Microarray data of genes downregulated in *TCP13pro::TCP13SRDX* transgenic plants.
997 **Table S3** Gene Ontology (GO) enrichment analysis of 555 genes downregulated in
998 *TCP13pro::TCP13SRDX* transgenic plants.
999 **Table S4** Analysis of the promoters of genes downregulated in *TCP13pro::TCP13SRDX*
1000 transgenic plants.
1001
1002 **FIGURE LEGENDS**
1003 **Fig. 1** Expression pattern of *TCP13* in wild-type (WT; Col-0) Arabidopsis plants under different
1004 abiotic stresses. (a) Phylogenetic analysis of Arabidopsis class II TCP proteins and
1005 representative members of *Antirrhinum majus* CINCINNATA (CIN) and CYCLOIDEA (CYC)
1006 (Luo *et al.* 1996) families. The phylogenetic tree was constructed using the neighbor-joining
1007 method with the MEGA X software (Kumar et al. 2018). Rice (*Oryza sativa*) class I TCPs,
1008 PROLIFERATING CELL FACTOR1 (PCF1), and PCF2 (Kosugi and Ohashi 2002) were used
1009 as an outgroup. The underlined names represent proteins containing the miR319A/JAW target
1010 sequence (Palatnik et al. 2003). Black dots indicate proteins involved in leaf differentiation
1011 (Koyama et al. 2007; Koyama et al. 2010). (b) Quantitative real-time PCR (qRT-PCR) analysis
1012 of the relative transcript levels of *TCP13, TCP5*, and *TCP17*. Plants were treated with water
1013 (control), dehydration stress, 10 μM abscisic acid (ABA), or salt stress (175 mM NaCl), and
1014 gene expression was examined at 3 and 6 h post-treatment. Data represent mean ± standard
1015 deviation (SD; $n = 3$). Asterisks indicate significant differences ($*p < 0.05$, $**p < 0.01$; one-way

ANOVA with Welch's *t* test). (c) Schematic showing the structure of the 1,000 bp promoter of *TCP13*, *TCP5*, and *TCP17*. Red and blue circles indicate the ABA-responsive element (ABRE)-related sequences (ACGTGG/T) (Busk and Pages 1998; Yamaguchi-Shinozaki and Shinozaki 2006) and GMSAUR (CATATG) motif found in the promoter of the soybean *SAUR15A* gene(Xu et al. 1997), respectively.

Fig. 2 Expression pattern of *TCP13* in Arabidopsis plants at different developmental stages, and subcellular localization of the TCP13 protein. (a–c) Histochemical staining showing β-glucuronidase (GUS) reporter activity (blue) under the control of the *TCP13* promoter in seedlings (a), leaves (b), and in an enlarged view of the true leaves (c). Scale bars = 1 mm (a and c); 5 mm (b). (d) Analysis of the relative transcript level of *TCP13* in leaves and roots by qRT-PCR. Transcript levels of genes were normalized relative to the constitutive control, *At2g32170* (Czechowski et al. 2005). Data represent mean ± SD (n = 3). (e) Subcellular localization of TCP13-sGFP fusion protein in Arabidopsis mesophyll protoplasts. Scale bars = 5 μm.

Fig. 3 Characterization of *TCP13* overexpression (*TCP13OX*) lines, *TCP13* repression (*TCP13SRDX*) lines and *tcp13* loss-of-function mutant plants at different developmental stages. (a) Root growth of 7-day-old *35Spro::TCP13OX* and *TCP13pro::TCP13SRDX* seedlings. Scale bars = 5 mm. (b and c) Hypocotyl (b) and root (c) length of 7-day-old *35Spro::TCP13OX* and *TCP13pro::TCP13SRDX* seedlings. Data represent mean ± SD (n = 6). An asterisk shows that the indicated mean is significantly different from the mean value of the control plant (**$P < 0.01$, ***$P < 0.001$; one-way ANOVA with Welch's *t* test). (d–h) Images of 14-day-old empty vector control (d), *35Spro::TCP13OX* (e), *35Spro::TCP13SRDX* (f), *TCP13pro::TCP13SRDX* (g), and *tcp5tcp13tcp17* (*tcp5/13/17)* triple knockout mutant (h) plants grown in agar. Scale bar = 5 mm (d, e, g, and h); 1 mm (f). (i–r) Images of 21-day-old *35Spro::TCP13OX* (i) and corresponding empty vector control (j) plants; 28-day-old *tcp13* mutant (k) and corresponding WT (l) plants; 28-day-old *TCP13pro::TCP13SRDX* (m and n) plants; 21-day-old *tcp5/13/17* (o) and corresponding WT (p) plants; and 28-day-old *tcp5/13/17* mutant (q) and corresponding WT (r) plants. Scale bars = 10 mm.

Fig. 4 Characterization of *TCP13OX* and *tcp13* mutant plants in the ABA treatment. Five-day-old seedlings were transferred to control and ABA-containing medium and grown for 7 days and root length was measured. Root elongation under the ABA treatment was compared with that under the control treatment, and the rate of root elongation was calculated. (a and b) Images of the root growth of *35Spro::TCP13OX* transgenic and control plants (a) and *tcp13*

mutant and WT plants (b) in the ABA treatment. Scale bars = 10 mm. (c) The root length of *35Spro::TCP13OX* transgenic and control plants (left panel) and *tcp1*3 mutant and WT plants (right panel) in the ABA treatment. (d) Relative level of root elongation of *35Spro::TCP13OX* transgenic and control plants (left panel) and *tcp1*3 mutant and WT plants (right panel) in the ABA treatment. In each transgenic or mutant plants, average of root length in the control condition was set to 100. Data represent mean ± SD (n =7). An asterisk shows that the indicated mean is significantly different from the mean value of the wild-type plant under the corresponding condition (***$P < 0.001$, one-way ANOVA with Welch's t test).

Fig. 5 Characterization of *35Spro::TCP13OX*, *tcp13* and *tcp5/13/17* mutant plants under osmotic stress conditions. Nine-day-old *35Spro::TCP13OX* and control plants, and *tcp13* mutant, *tcp5/13/17* mutant and WT plants were transferred to 1/2 MS medium containing 25 mM mannitol for 13 days. The leaf area of third (L3), fourth (L4), and fifth (L5) leaves was measured. Leaf growth under the mannitol treatment was compared with that under the control treatment, and the rate of leaf growth was calculated. (a and d) Images of cotyledon (C) and true leaves (L) of *35Spro::TCP13OX* and control plants (a) and *tcp13* mutant, *tcp5/13/17* mutant and WT plants (d) exposed to control and mannitol treatments. Scale bars = 5 mm. . (b and e) The leaf area in *35Spro::TCP13OX* transgenic and control plants (b) and *tcp13* mutant, *tcp5/13/17* mutant and WT plants (e) treated with control and mannitol medium. (c and f) Relative level of leaf growth in *35Spro::TCP13OX* transgenic and control plants (c) and *tcp13* mutant, *tcp5/13/17* mutant and WT plants (f) treated with mannitol. In each transgenic or mutant plants, average of leaf area in the control condition was set to 100. Data represent mean ± SD (n = 5). An asterisk shows that the indicated mean is significantly different from the mean value of the wild-type plant under the corresponding condition (*$P < 0.05$, **$P < 0.01$, ***$P < 0.001$; one-way ANOVA with Welch's t test).

Fig. 6 Characterization of *35Spro::TCP13OX* plants under severe dehydration stress. *35Spro::TCP13OX* and control plants were grown in soil for 14 days with well-water conditions. One pot contained 5 plants of each line. 9 pots of *35Spro::TCP13OX* 35S*a* and *b*, and 18 pots of control plants were transferred to empty tray and exposed dehydration stress by withholding watering for 14 days. After dehydration treatment, plants were grown for 7 days with well-water conditions and evaluated the survival rate of plants. (a) Images of plants before dehydration stress (Untreated) and after dehydration (Dehydration). The survival rate of plants is indicated below the images. Scale bars = 10 mm. (b) Water loss assay of detached leaves of 5-week-old *35Spro::TCP13OX* 35S and control plants. The *nced3-2* plants represent a negative control. Data represent mean ± SD (n = 4). An asterisk shows that the indicated mean is significantly

different from the mean value of the control plant under the corresponding condition (*$P < 0.05$, **$P < 0.01$, ***$P < 0.001$, one-way ANOVA with Welch's *t* test).

Fig. 7 Transcriptome analysis of genes downregulated in *TCP13pro::TCP13SRDX* plants. (a) GO enrichment analyses of downregulated in *TCP13pro::TCP13SRDX* plants. (b) Venn diagram showing the overlap between genes downregulated in *TCP13pro::TCP13SRDX* plants and those upregulated by dehydration stress (Urano et al. 2017). (c–e) Relative transcript levels of downregulated genes including ABA- and dehydration-inducible genes (c), *CIN-like TCP* common downstream genes involved in auxin signaling (d), and flavonoid biosynthesis genes (e) in *TCP13pro::TCP13SRDX* plants. Data represent mean ± SD ($n = 4$). (f) Enrichment of hexamer motifs in the promoter regions (~1,000 bp) of downstream candidate genes of *TCP13*. Hexamer motifs in the promoter regions of the top 100 downregulated genes in *TCP13pro::TCP13SRDX* plants were analyzed as described previously (Maruyama et al. 2012). (g) Comparison of TCP binding and ABRE motifs identified in the promoter regions of downregulated genes in *TCP13pro::TCP13SRDX* plants. (h) Comparison of the 1,000 bp promoter regions of *TCP13SRDX*-downregulated genes with those of 23,739 Arabidopsis genes used previously for motif analyses (Maruyama et al. 2012) by χ^2 tests. ACGTGT and ACGTGG were used as the ABRE sequences, and GGACCA and TGGTCC were used as the TCP binding motifs. Significant differences between the observed and expected values of the frequency of overlap between the ABRE and TCP binding motifs (**$p < 0.01$, ***$p < 0.001$).

Fig. 8 Expression analysis of *TCP13* downstream genes in *tcp13* mutant plants under dehydration stress. (a and b) Expression of common downstream target genes of CIN-like TCPs (a), and expression of ABA-inducible genes (b) analyzed by qRT-PCR. Transcript levels of genes were normalized relative to the constitutive control, *At2g32170* (Czechowski et al. 2005). In each experiment, the maximum gene transcript level was set to 100. Data represent mean ± SD ($n = 3$ technical replicates). An asterisk shows that the indicated mean is significantly different from the mean value of the wild-type plant under the corresponding condition (*$P < 0.05$, one-way ANOVA with Welch's *t* test).

Fig. 9 Protoplast transient assays of ABA- and auxin-regulated genes in *tcp13* mutant plants. (a) Existence of the ABREs (ACGTGT, ACGTGG, ACACGT, and CCACGT), AuxREs (TGTCTC and GAGACA), and TCP binding motifs (GGACCA, GGTCCT, TGGTCC, and AGGACC) in *AHG3*, *Gols2*, *IAA5*, and *LBD1* promoters. The *LBD1* promoter also contained the TCP binding motif like (TGGTCA). (b and c) Protoplast transient assays for the activation analysis of ABA-regulated genes (b) and auxin-regulated genes (c) in WT and *tcp13* mutant

protoplasts in response to 5 μM ABA or 1 μM IAA. In each experiment, relative luciferase (LUC) activity in the control condition was set to 100. Data represent mean ± SD (n = 3 technical replicates). An asterisk shows that the indicated mean is significantly different from the mean value of the wild-type plant under the corresponding condition (*$P < 0.05$, **$P < 0.01$, one-way ANOVA with Welch's t test).

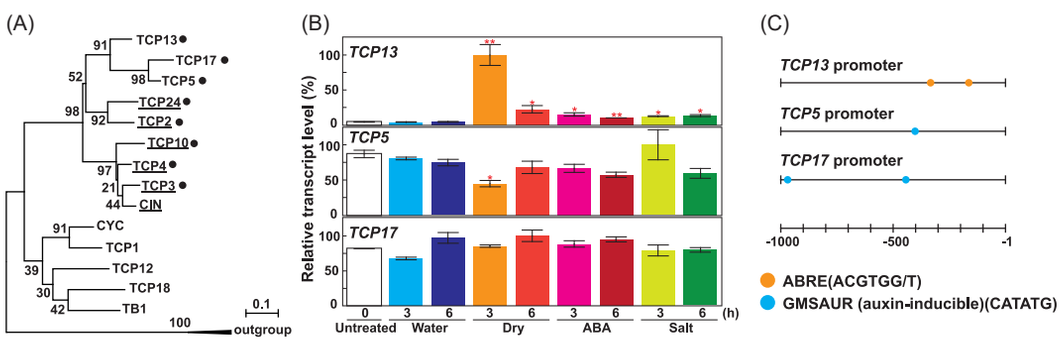

(Urano *et al.*, Figure 1)

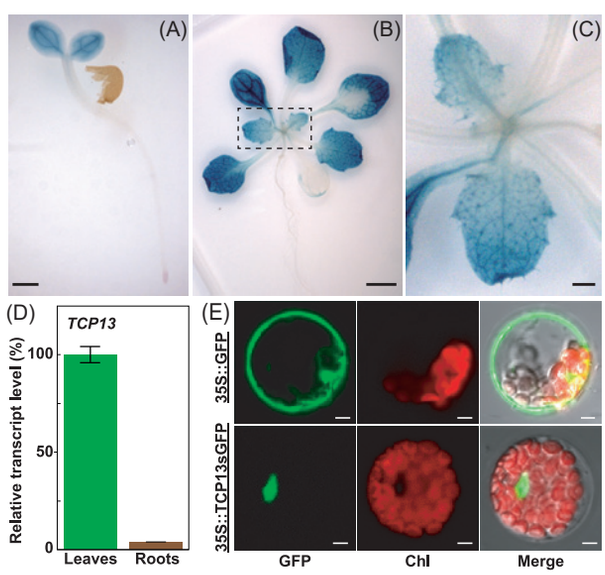

(Urano *et al.*, Figure 2)

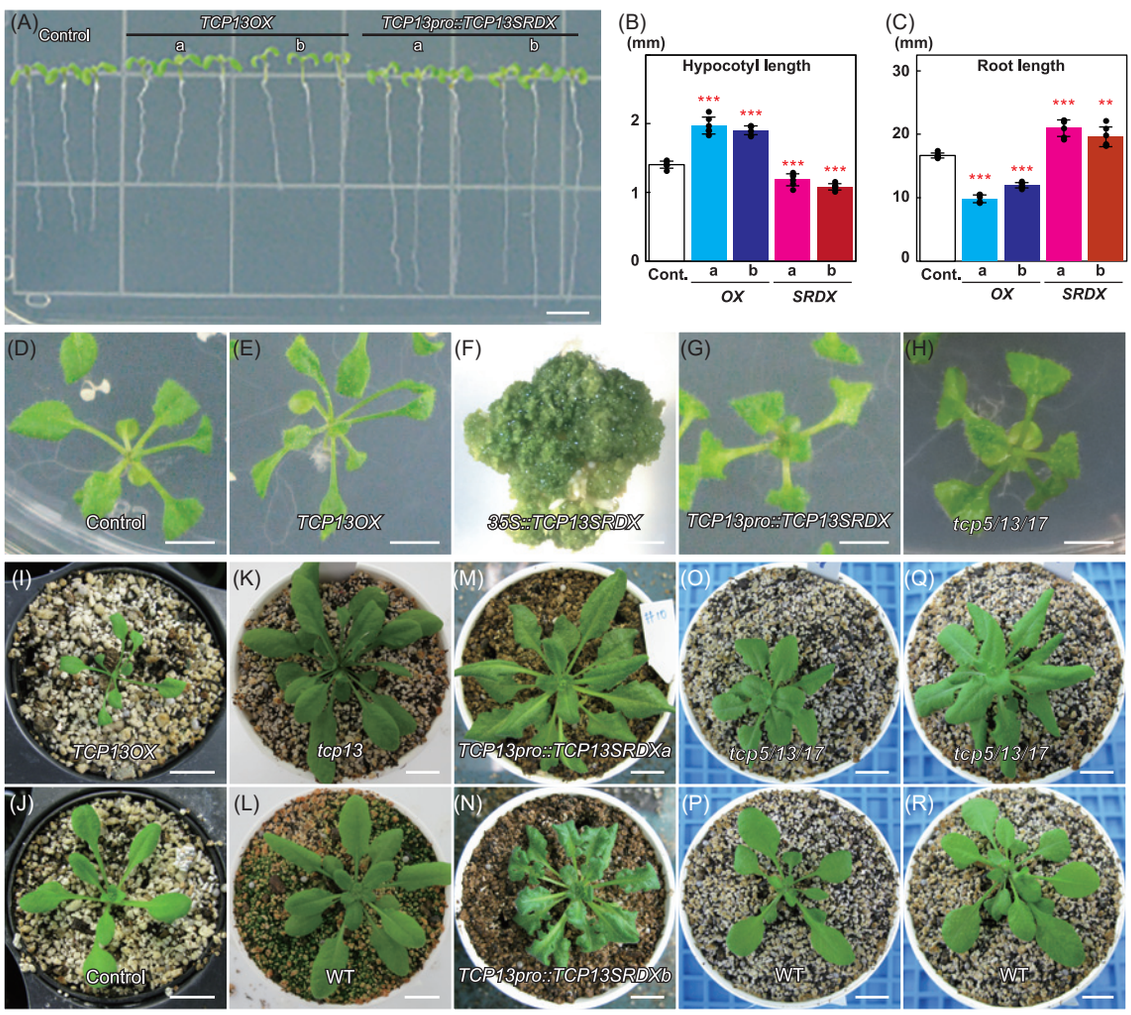

(Urano *et al.*, Figure 3)

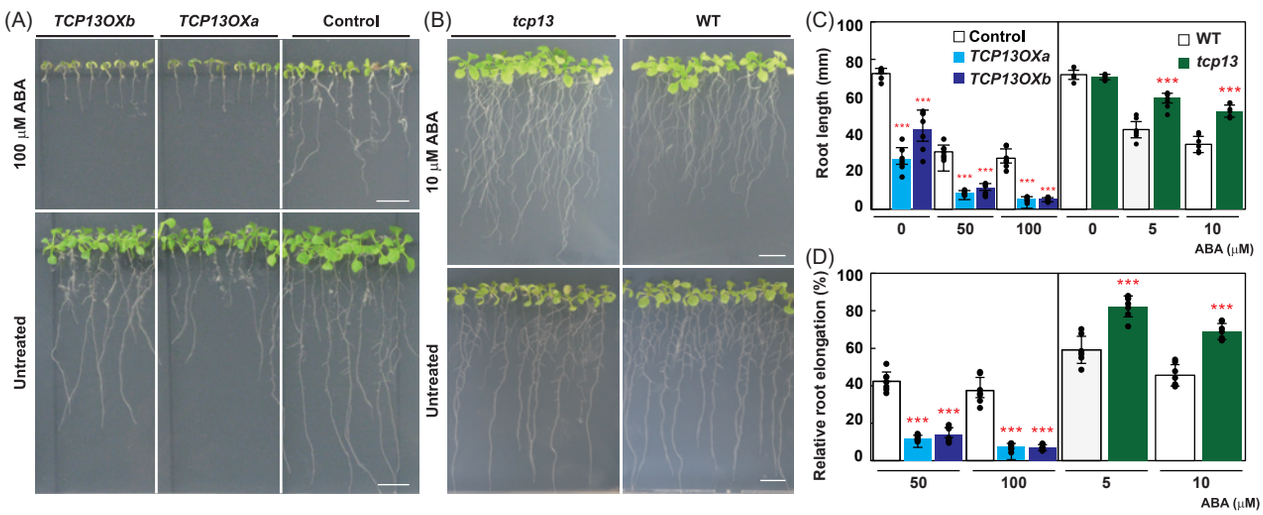

(Urano et al., Figure.4)

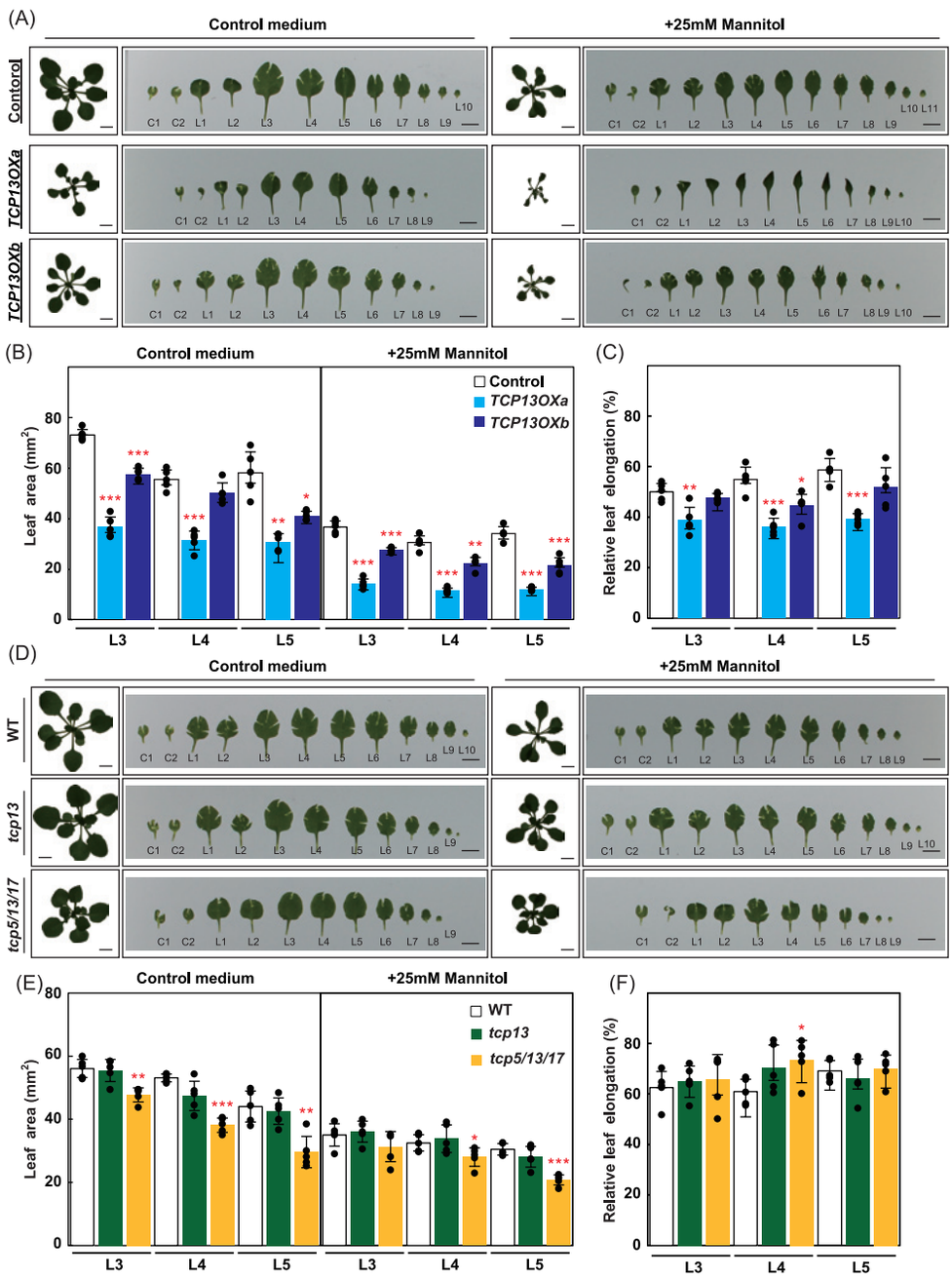

(Urano *et al.*, Figure 5)

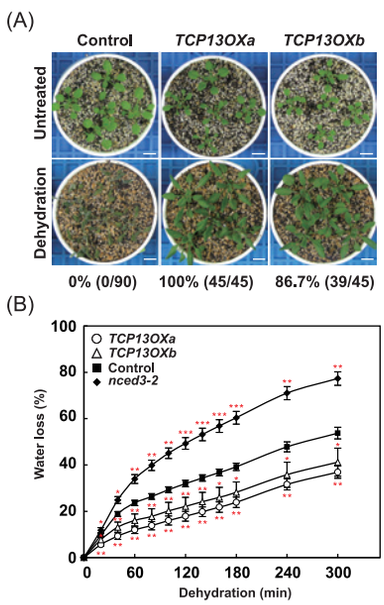

(Urano *et al*., Figure 6)

(A)

GO of genes downregulated in *TCP13SRDX*

GO biological process	Gene number	-P
response to stimulus	202	17.4
response to abiotic stimulus	108	15.9
response to chemical	126	15.8
response to stress	125	10.5
response to endogenous stimulus	74	10.1
response to hormone	73	9.9
response to oxygen-containing compound	78	9.9
response to organic substance	84	9.8
response to acid chemical	59	7.0
response to osmotic stress	37	6.1

1 <20

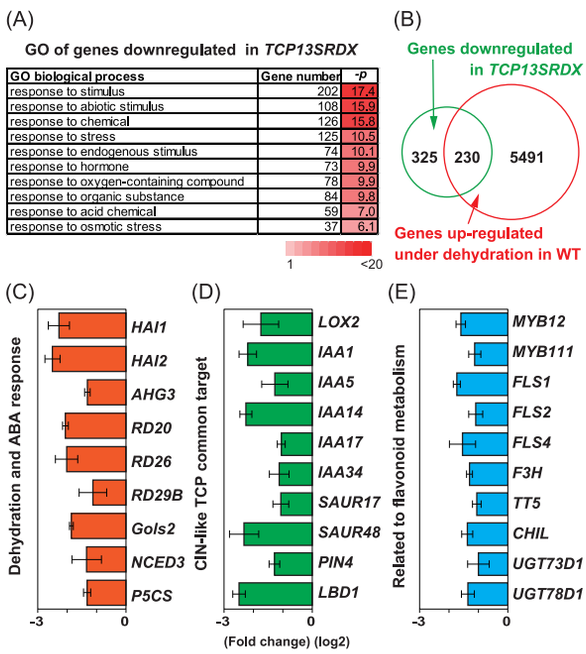

(F)

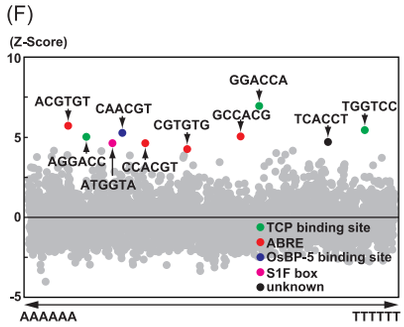

(G)

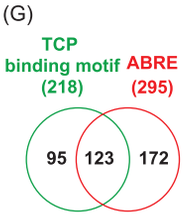

(H)

Combination of ABRE and TCP binding motif		TCP13SRDX-down regulated genes		23739 genes		X^2 test	
ABRE	TCP binding motif	Expected Value	Found value	Expected Value	Found value	*p*-value	
ACGTGT	GGACCA	22.16	47	566.8	542	7E-09	***
ACGTGT	TGGTCC	9.71	35	248.3	223	1.2E-18	***
ACGTGG	GGACCA	15.50	34	418.5	400	2.7E-07	***
ACGTGG	TGGTCC	16.14	26	435.9	426	7.1E-03	**

(Urano *et al.*, Figure 7)

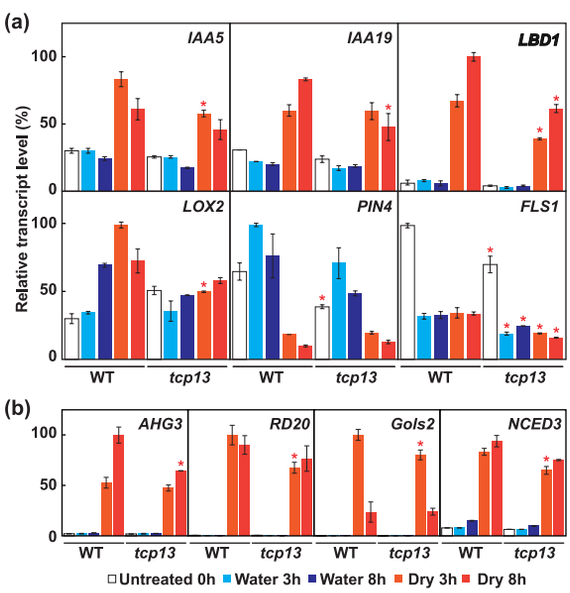

(Urano *et al*., Figure 8)

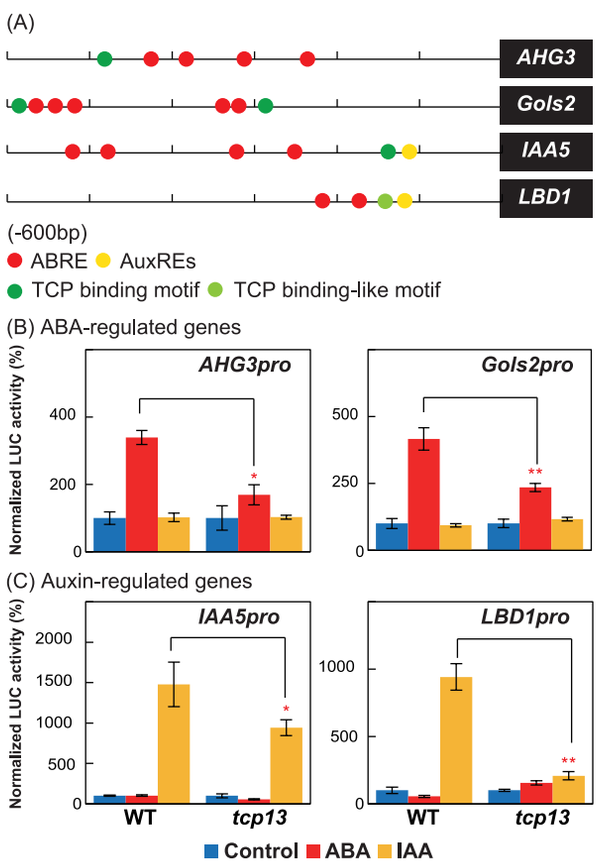

(Urano *et al.,* Figure, 9)

Supplementary Files

This is a list of supplementary files associated with this preprint. Click to download.

- Uranoetal.SIFigures.pdf
- Uranoetal.SupportingExperimentalProcedures.pdf
- Uranoetal.TableS1.xlsx
- Uranoetal.TableS2.xlsx
- Uranoetal.TableS3.xlsx
- Uranoetal.TableS4.xlsx